Marine and Petroleum Geology 128 (2021) 105061

Contents lists available at ScienceDirect

Marine and Petroleum Geology

journal homepage: www.elsevier.com/locate/marpetgeo

Research paper

Maturity evolution of Lower Cambrian Qiongzhusi Formation shale of the Sichuan Basin

Qiu Nansheng [a,b,*], Liu Wen [a,c], Fu Xiaodong [d], Li Wenzheng [d], Xu Qiuchen [a], Zhu Chuanqing [a,b]

[a] State Key Laboratory of Petroleum Resources and Prospecting, China University of Petroleum, Beijing, 102249, China
[b] College of Geosciences, China University of Petroleum, Beijing, 102249, China
[c] Institute of Geomechanics, Chinese Academy of Geological Science, Beijing, 100081, China
[d] PetroChina Hangzhou Research Institute of Geology, Hangzhou, 310023, China

ARTICLE INFO

Keywords:
Maturity evolution
Lower Cambrian Qiongzhusi formation shale
Thermal history
Sichuan basin

ABSTRACT

The Lower Cambrian Qiongzhusi Formation source rock is one of the main sources of oil and gas in the Sichuan Basin. Owing to the controversial thermal history and the complex structural pattern in the Sichuan Basin, it is difficult to characterize the differences in maturity evolution and the timing of hydrocarbon generation periods of Qiongzhusi hydrocarbon source rocks in different tectonic zones. Based on the comprehensive analysis of the previous thermal history and denudation studies from the tectonic units of the basin, the thermal histories and denudation amount in main period of tectonic movement of a five-part tectonic development are obtained in this paper. Although the thermal history of different tectonic units varies, generally, the heat flow increased slowly in the early Paleozoic, and it experienced a peak heat flow at the end of the Middle Permian and decreased subsequently. Based on new thermal history and denudation data, the maturation of the Lower Cambrian Qiongzhusi Formation source rocks in the Sichuan Basin were modeled and their evolution can be classified into three patterns, which are: (1) continuous heating pattern in southern Sichuan, (2) Silurian-Permian heating cessation pattern in western Sichuan and northwest central Sichuan, and (3) Silurian-Permian and Triassic heating cessation pattern in the central uplift, northern structural zone and western part of the eastern structural zone. In addition, the key hydrocarbon generation periods of different tectonic units were determined in this study. Tectonic and sedimentary burial, together with high heat flow values during the Late Permian, were the main factors controlling levels of thermal maturity and thermal evolution models of the Qiongzhusi Formation. The present-day thermal maturity of the Qiongzhusi Formation depends on the thermal history and maximum burial depth before uplift in Late Cretaceous. However, the maturity evolution pattern affecting the key hydrocarbon generation stage was mainly related to the burial histories of source rocks in the Paleozoic. The thermal modelling of this study provides new evidence for the source rock evolution and new insight into Lower Paleozoic shale gas.

1. Introduction

Recently, great breakthroughs have been made in the natural-gas exploration in the succession of the Sinian and Lower Paleozoic strata in the Sichuan Basin. Therefore, the marine source rocks of these ancient strata in southern China are of high interest. Furthermore, the hydrocarbon (HC) generation potential of over-mature source rocks has received increased attention (Wang et al., 2017; Luo et al., 2017). The Lower Cambrian Qiongzhusi Formation source rock is one of the main sources of oil and gas in the Sichuan Basin (Li et al., 2016; Wei et al., 2015; Du et al., 2016). However, the burial evolution of the Qiongzhusi Formation is complex and the maturities of this source rock vary widely among different tectonic units. The early Paleozoic thermal history is controversial since only bitumen reflectance and vitrinite-like reflectance were used to calibrate thermal models in prior studies. The critical periods of the hydrocarbon generation threshold and oil and gas generation peaks in different areas are therefore unknown. This restricts the allocation evaluation of hydrocarbon accumulation factors for this critical period.

The thermal evolution of Cambrian source rocks in the Sichuan Basin mainly presents the characteristics of a multiphase evolution. There are two different patterns for the thermal evolution of Lower Paleozoic

* Corresponding author. State Key Laboratory of Petroleum Resources and Prospecting, China University of Petroleum, Beijing, 102249, China.
E-mail address: qiunsh@cup.edu.cn (Q. Nansheng).

https://doi.org/10.1016/j.marpetgeo.2021.105061
Received 28 September 2019; Received in revised form 23 August 2020; Accepted 26 March 2021
Available online 1 April 2021

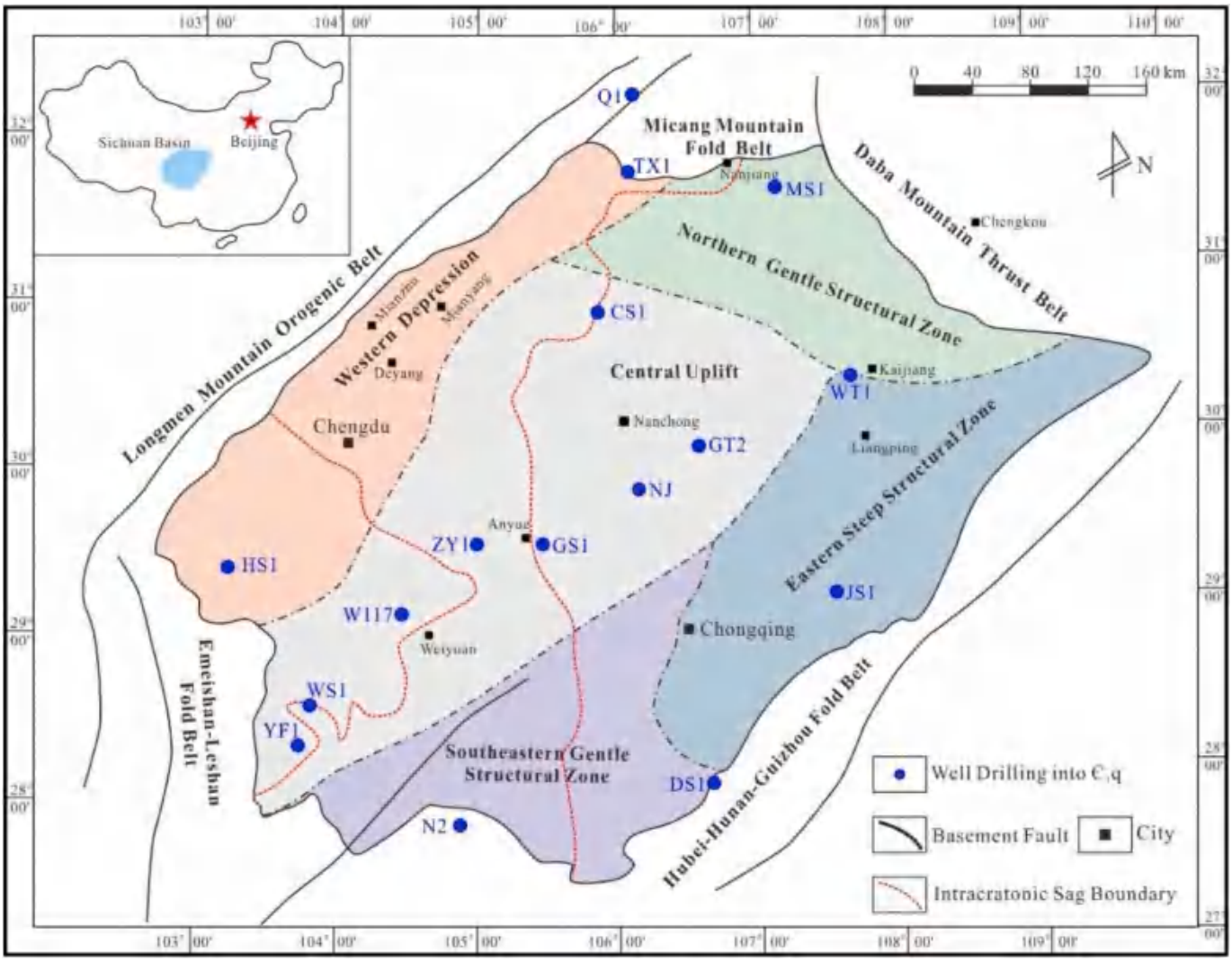

Fig. 1. The division of structural units in Sichuan Basin (modified after Zhu et al., 2015) and the study well locations in this paper.

source rocks: ① the Sinian-Permian early-mature stage, Permian-Triassic middle-mature stage, Jurassic rapid-mature stage and Cretaceous-Tertiary late-mature stage and ② immature in the Caledonian tectonic period, and a rapid evolution and conclusion during the Permian, or a continuous maturation during the Late Hercynian-Yanshanian Period (Zhang et al., 2007a; Xu et al., 2018). Consequently, variance in maturity patterns is evident in different tectonic units. Some studies show that the thermal evolution of the Lower Paleozoic source rocks in central and southern Sichuan belongs to the Permian rapid evolution, whereas eastern and northeastern Sichuan are characterized by a multi-stage evolution (Xu et al., 2007; Zhang et al., 2007b). Rao et al. (2013) established four thermal evolution models for Sinian-Lower Paleozoic source rocks in the Sichuan Basin based on an analysis of the differences in the sedimentary models of different tectonic units and the effect of the tectono-thermal evolution on the maturity of source rocks. The four thermal evolution patterns of the Lower Cambrian and Lower Silurian source rocks include: (1) HC generation during Caledonian period, then ceased after rapid secondary maturation at the end of the Early Permian, (2) immature at the end of Caledonian period, then rapid evolution and cessation at the end of Early Permian, (3) two evolution stages at the Caledonian and Hercynian-Yanshanian periods, and (4) continuous evolution that lasted from Late Permian to the Yanshanian.

There are many scenarios for the characteristics of thermal evolution in Lower Paleozoic source rocks in the Sichuan Basin (Wei et al., 2013). However, publications on the thermal evolution of these source rocks are controversial. The reported key hydrocarbon generation periods of the source rocks in the same strata and area differ between researchers and therefore provide no clear guidance for exploration. The reason behind the different interpretation of source rock evolution is that there are disputes on the understanding of basin thermal history, tectonic uplift and denudation of the basin. This can be attributed to the fact that Since the Sichuan Basin is a superimposed petroleum basin that experienced poly-phase fold-and-thrust tectonic evolution stages (Li et al., 2006), which resulted in a complicated thermal history. Recently, there is a wide literature on the thermal history reconstruction of the superimposed basin or fold-and-thrust belts by the thermal indicators of vitrinite reflectance and low temperature thermochronology (Qiu et al., 2012; Rojas et al., 2015; Zhu et al., 2016; Aldega et al., 2018; Schito et al., 2018; Nielsen et al., 2017; Peters et al., 2018; Balestra et al., 2019a, 2019b; Omodeo et al., 2019). Hence, the thermal history is the key problem restricting the study of the hydrocarbon source rock evolution. Thermal history of the Sichuan Basin has been investigated by many researchers (e.g. Qiu et al., 2008; He et al., 2011b, 2014; Ma et al., 2012; Huang et al., 2012; Zhu et al., 2015; Cao et al., 2016; Xu et al., 2018; Liu et al., 2018), however, most of these studies are mainly aimed at one or a few of the tectonic units of the basin. Moreover, thermal maturity analysis of the Cambrian Qiongzhusi Formation has only

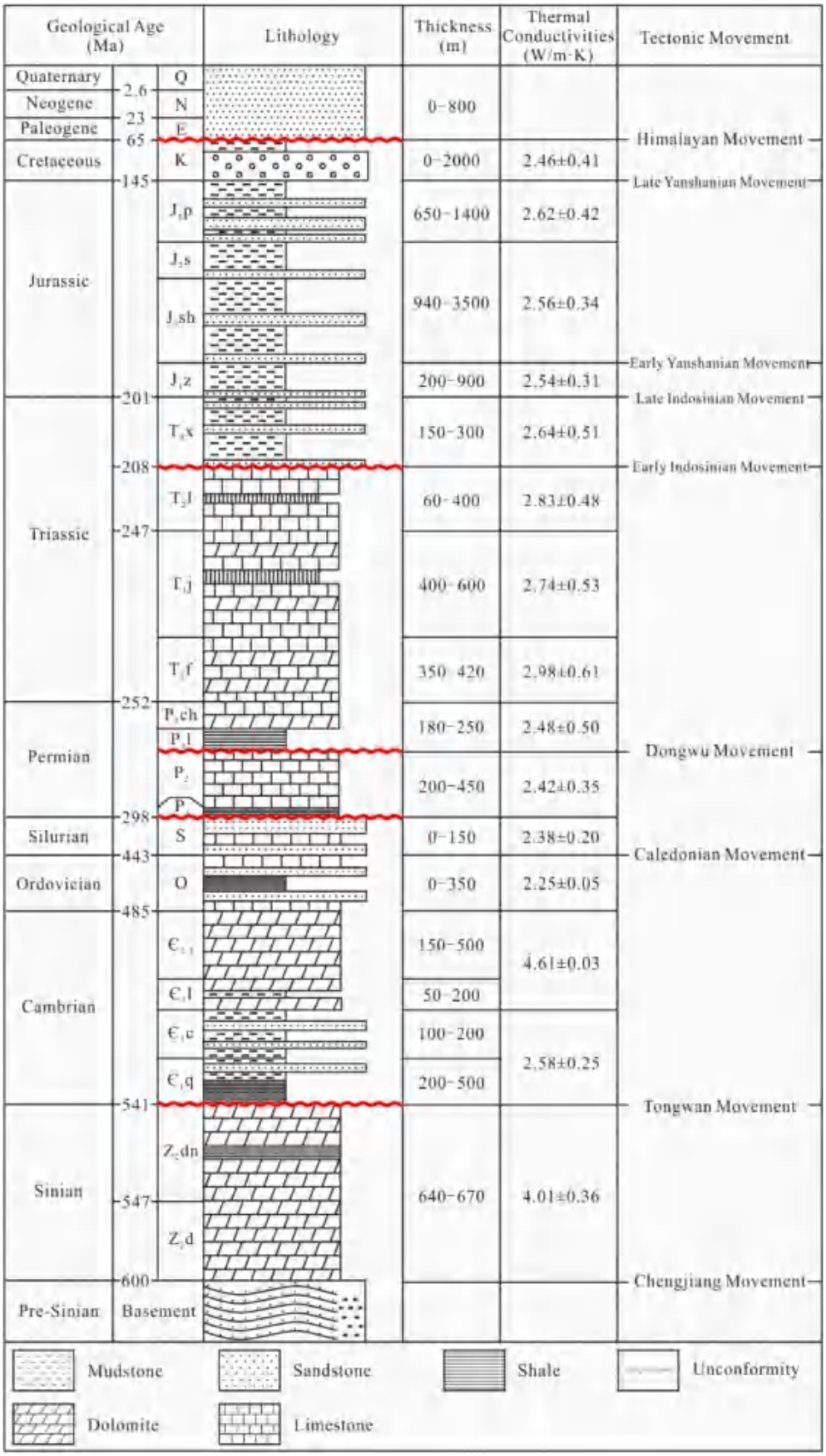

Fig. 2. The composite columnar section of lithology (modified after Liu et al., 2016).

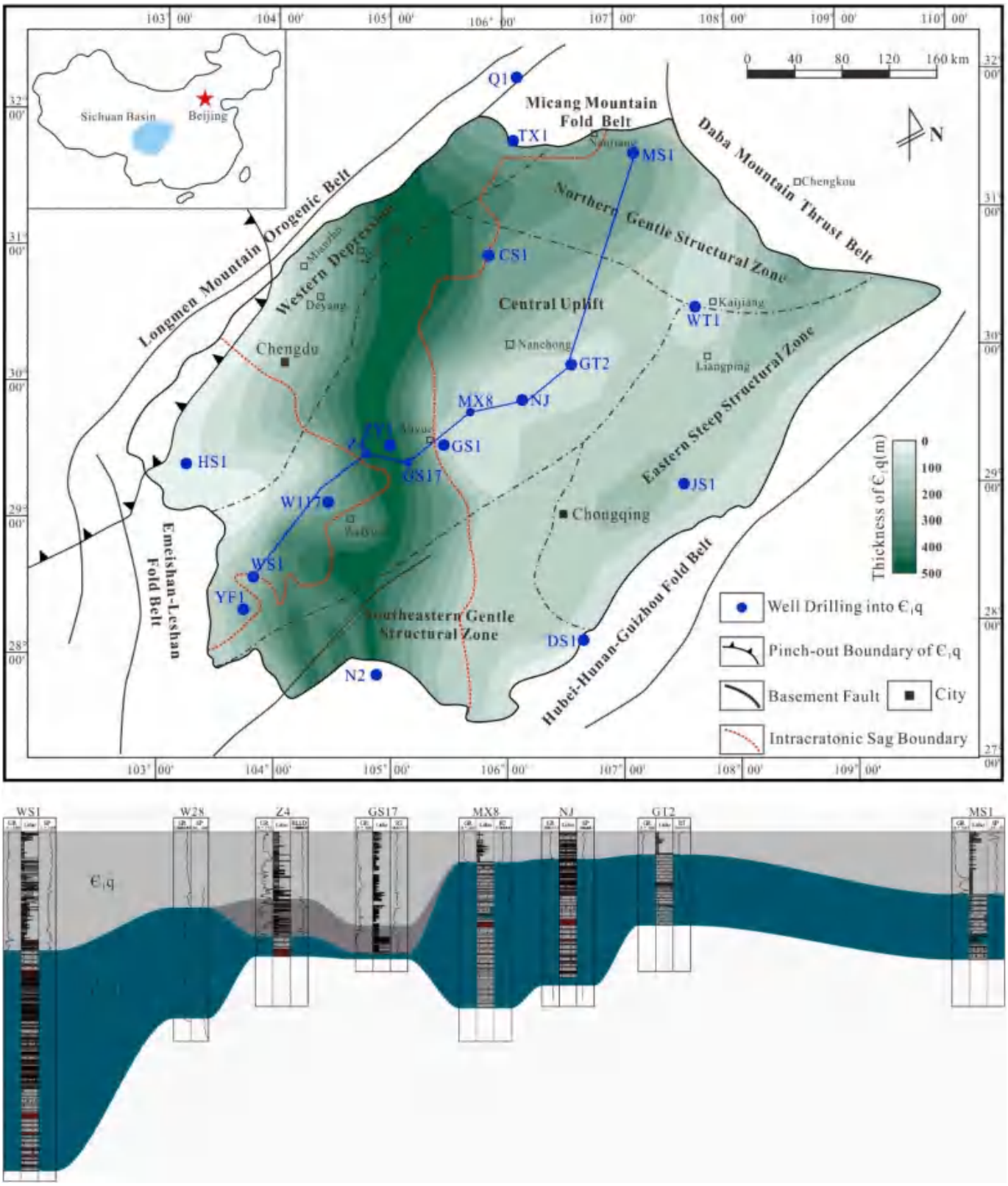

Fig. 3. a. The thickness distribution of effective source rock in $\epsilon_1 q$ (modified after Zhao et al., 2020); b. Stratigraphic correlation from well WS1, GS17 to MS1.

focused on localized areas of the basin. Based on the comprehensive analysis of these local data, the thermal history of the major tectonic units has been obtained in our study. Thermal evolution processes of Lower Cambrian source rocks in different tectonic units are simulated and different evolutionary patterns are established systematically in this paper, based on these latest data of the thermal history and denudation of different tectonic units in the Sichuan Basin. The Cambrian Qiongzhusi Formation is one of the most important source rocks in the Sichuan Basin, and this study clarifies its maturation history, provides new evidence for oil and gas accumulation and insights into the Lower Paleozoic

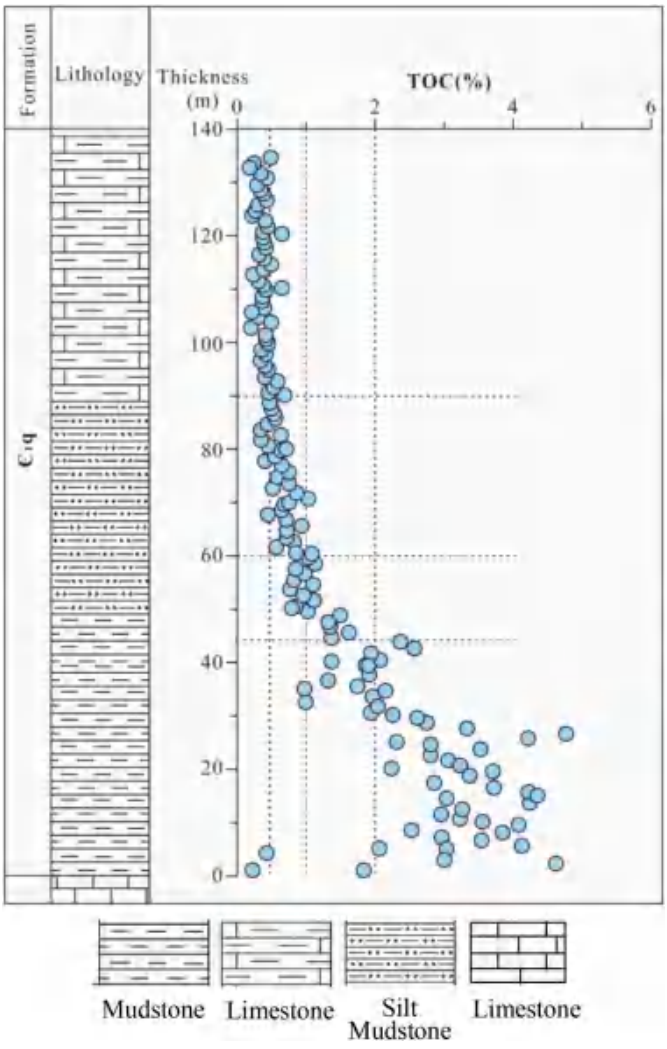

Fig. 4. The source rock profile of the Lower Cambrian Qiongzhusi Formation in the Nanjiang profile in northern Sichuan (Liang et al., 2008).

shale gas.

2. Geological setting

2.1. Tectonic evolution of Sichuan Basin

The Sichuan Basin—a large, superimposed petroleum basin—is located in the northwest of the Upper Yangtze Craton in southwest China. The basin developed from a passive continental margin basin—a superimposed Mesozoic-Cenozoic foreland basin—of Sinian–Mesozoic strata (Li et al., 2006). The Sinian period was the formation stage of the Sichuan Basin. In the early basin development stage, sedimentation has the function of filling and leveling. With the erosion of the peripheral basin margins, sandstone, shale, and other siliciclastic rocks were unconformable deposited on the west-inclined basement of the Yangtze Plate. At the end of the Sinian, the Tongwan Orogeny led to a large uplift and denudation, and the basin morphology changed. From the Cambrian to the Silurian period, before the Caledonian tectonism, the initial stage of deposition and evolution of the Qiongzhusi Formation occurred. During the Cambrian-Ordovician period, with the further breakup of the Rodinia supercontinent, the basement of the Yangtze Plate was tilted toward the southeast. Thus, the Sichuan-Yunnan region in the west and the Micang Mountain to the north were uplifted; the central region was a flat platform, and the eastern region was a slope (Wang et al., 2015).

Because the Upper Yangtze Plate has long maintained its transitional position between the Gondwana and Loya Continents (Ren et al., 2016), the basin exhibits strong tectonic activity. The present situation of the Sichuan Basin was formed by inheritance and development of the Yanshanian Orogeny and strong transformation during the Himalayan Orogeny, according to the structural framework provided by the Indo-Chinese Movement. Based on the lithology of the basement, distribution of caprocks, and degree of deformation, the basin is classified into five tectonic units: western depression, northern gentle structural zone, eastern steep structural zone, southeastern gentle structural zone and central uplift (Fig. 1). Before the Middle Triassic, marine deposits of the craton basin dominated the Sichuan Basin (Ma et al., 2007), and the basin experienced the Tongwan, Caledonian, Dongwu and Indosinian Tectonism. Owing to the extrusion of the Tethys and Pacific Plates, the Sichuan Basin exhibited its present-day rhombic basin shape by the Middle Triassic. Fluvio-lacustrine continental deposits occurred in the Sichuan Basin, owing to seawater withdrawal since the Late Triassic. Subsequently, 3000–4000 m of continental siliciclastic rocks were deposited in the basin since the Late Triassic. However, affected by Himalayan tectonic, the plate margin was strongly reshaped during the late orogenic deformation, and most continental strata were eroded (Robert et al., 2010; Zou et al., 2014a). As a whole, the Sichuan Basin has experienced three tectonic development stages: marine carbonate platform from Sinian to Late Triassic, continental basin from Late Triassic to Eocene, and folding & uplift since Oligocene (Li et al., 2006; He et al., 2011a, b; Liu et al., 2012, 2017). The basin experienced four periods of uplift and denudation from Cambrian to present-day, and multiple unconformities developed in the stratigraphy as a consequence (Liu et al., 2016) (Fig. 2). The composite stratigraphic section shows the vertical distribution of sedimentary characteristics in Sichuan Basin (Fig. 2).

2.2. Source rock characteristics of Lower Cambrian Qiongzhusi Formation

The Cambrian stratum is widely distributed in the northern and southern slopes of the Central Uplift, the northern part of the western depression, and the eastern Sichuan Slopes. The hydrocarbon source rocks occur mainly in the Lower Cambrian Qiongzhusi Formation ($Є_1q$) as a combination of black mudstone, shale, and grey silty mudstone with type I marine organic matter (Zou et al., 2014b; Li et al., 2016). Fig. 3 shows the thickness distribution of effective source rock in $Є_{1q}$, and a SW-NE stratigraphic correlation shows thickness and lithological variations of Cambrian Qiongzhusi Formation. In the central uplift, the thickness of Cambrian Qiongzhusi Formation decreases from southwest to northeast (Fig. 3b). There are abundant source rocks composed of pure mudstones, which developed in the lower part of the profile. The TOC content decreases as silt and calcite increase in the upper part of the profile. For example, TOC content from outcrop samples at the base of the profile of the Nanjiang profile in northern Sichuan is 4%–5%. In contrast, mudstones 60 m above the bottom contains silt and TOC <1%, and black mudstone 90 m above the bottom contains calcite with TOC <0.5%; neither lithology is classified as a hydrocarbon source rock (Fig. 4).

The effective source rocks of the Qiongzhusi Formation in the Sichuan Basin and its adjacent areas are approximately 50–450 m thick and exhibit three depocenters (Zou et al., 2014a). ① Deyang-Anyue Rift area. The thickness of the effective source rocks in the northern section of the rift depression is the highest, typically 200–450 m. Secondary rifts developed on the northern slope of the central Sichuan Paleo-uplift have source rocks 150–300 m thick. In the south part of the Deyang-Anyue rift trough, the thickness is slightly reduced (approximately 100–400 m). ② Chengkou area, northeast Sichuan. The thickness of the effective source rocks is in the range of 150–250 m, and the depocenter can extend into the basin of the Kaijiang-Liangping area. ③ Wufeng-Xiushan area. This area is located outside of the east of Sichuan Basin. The thickness of the effective source rocks is 100–250 m. Affected by the Caledonian central

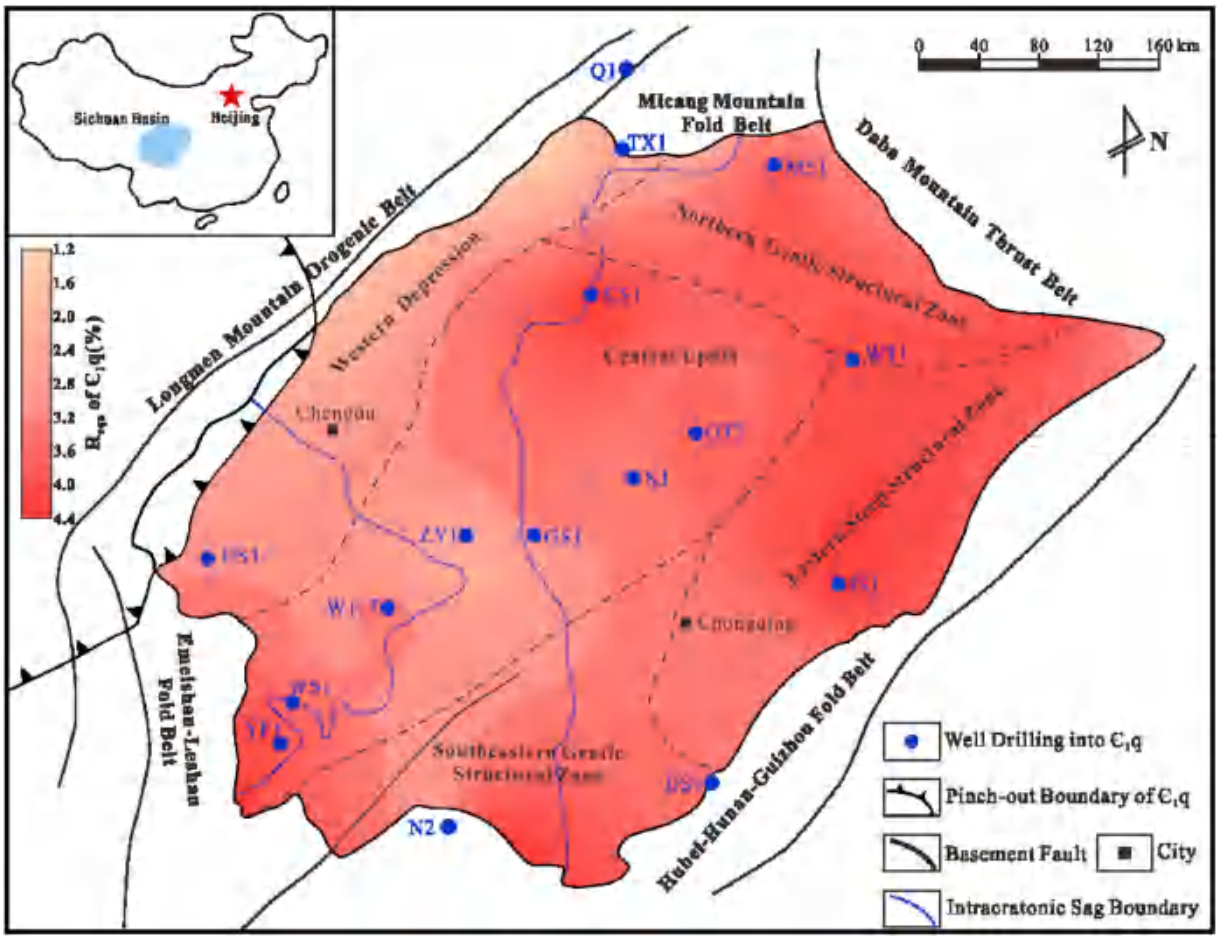

Fig. 5. The present-day's maturation distribution of the top Qiongzhusi Formation source rock in the Sichuan Basin.

Sichuan Paleo-uplift, northern Sichuan Paleo-continent, and submarine highlands, the thickness of the effective source rocks in the central basin, northern basin, and eastern margin of the basin are relatively low, typically 50–150 m thick) and effective source rocks do not occur in some areas.

The present-day maturity distribution map, based on equivalent-vitrinite reflectance (R_{equ}) data, converted from bitumen and graphite reflectance and provided by the Southwest Oil and Gas Field Branch, CNPC, indicates that the source rocks of the Qiongzhusi Formation are high-to over-mature in the entire basin, except for the late-mature zone around well ZY1 in the southwest of the basin (Fig. 5). There are two northwest–southeast maturity centers in the northeastern and south-western basin ($R_{equ} > 4\%$). However, the maturity is relatively low in the central Sichuan Paleo-uplift and piedmont zone of the western Sichuan depression. R_{equ} is 2.0%–3.2% and has reached the over-mature stage of dry-gas generation.

3. Methods and parameters

The parameters important for the source rock evolution include the thermal history, erosion amount, strata denudation process, thermo-physical parameters of the rocks, geochemical data of the source rocks, stratigraphic thickness, stratigraphic age, and lithological data.

3.1. Thermal history

Many studies on the thermal history of the Sichuan Basin have been conducted based on various thermal indicators (e.g. vitrinite reflectance, bitumen reflectance, and apatite fission track data) and geodynamic methods (Lu et al., 2006; Qiu et al., 2008; He et al., 2011b, 2014; Huang et al., 2012; Ma et al., 2012; Jiang et al., 2015; 2018; Zhu et al., 2010; 2015; 2016; Cao et al., 2015; Liu et al., 2018; Xu et al., 2018). In general, the basin was a stable craton before the Permian, and its thermal state was stable and exhibited a heat flow of 45–55 mW/m^2 with variability spread among the different tectonic units. During the Permian, a short peak-heat flow period occurred, which may have resulted from the thinning of the crust and Emeishan mantle plume activity. The thermal evolution of the five tectonic units in the Sichuan Basin was determined based on the heat flow evolution of typical wells by the above-referenced studies (Fig. 6). The heat flow value was approximately 50–55 mW/m^2 in the Early Paleozoic in the western depression. A peak heat flow of 85–90 mW/m^2 occurred at the end of the Middle Permian in the north part of the depression, but the peak heat flow exceeded 110 mW/m^2 in the south part of the depression (Well H-1). Subsequently, the heat flow decreased rapidly (Fig. 6a). The Early Paleozoic heat flow of the Central Uplift was 55–60 mW/m^2; The Central Uplift experienced a peak heat flow of 90 mW/m^2 at the end of the Middle Permian and decreased subsequently (Fig. 6b).

In the Early Paleozoic, heat flow of approximately 45 mW/m^2 occurred in the northern gentle structural zone. Furthermore, a peak heat flow occurred at approximately 260 Ma, and the maximum exceeded 70 mW/m^2 (Fig. 6d). However, this peak heat flow is much lower than that of the western depression and the central uplift. The heat flow has decreased since the Late Permian. The heat flow evolution in the eastern steep structural zone is similar to that in the northern gentle structural zone (heat flows of approximately 50 mW/m^2 during the Early Paleozoic and 60–80 mW/m^2 at the end of the Middle Permian) (Fig. 6c). The heat flow in the southeastern gentle structural zone is

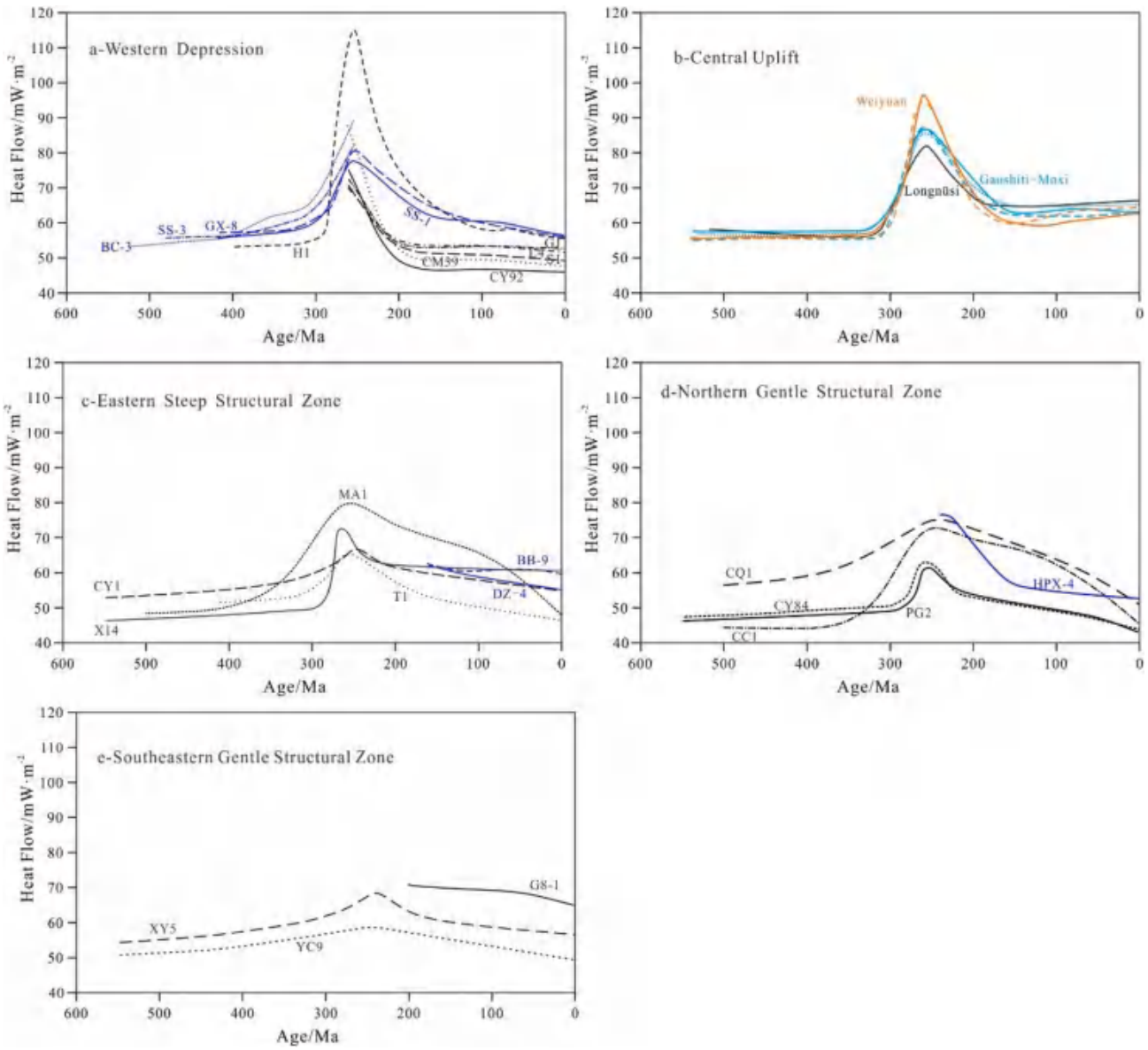

Fig. 6. Heat flow evolution in the different tectonic units in the Sichuan Basin.

relatively stable and exhibits slight fluctuations. The heat flow increased slightly in the Middle and Late Permian and then decreased to 50–60 mW/m^2 (Fig. 6e).

3.2. Erosion amount

In this study, the erosion data were obtained based on the following three main sources: ① Published documents (He et al., 2011a, b; Xu et al., 2012; Deng et al., 2013; Mei et al., 2014; Li et al., 2015; Jiang et al., 2018), ② the authors' previous research results in the Sichuan Basin (Qin et al., 2008; Qiu et al., 2008; Tian et al., 2012,2018; Zhu et al., 2009,2013,2016,2017,2019; Jiang et al., 2015; Cao et al., 2016; Liu et al., 2018; Xu et al., 2018), and ③ stratigraphic correlation between boreholes. The basin mainly experienced four main periods of uplift and denudation, at the end of the Early Paleozoic, in the Early to Middle Permian, in the Middle-Late Triassic, and during the Cretaceous to Neogene, which correspond to the Caledonian, Dongwu, early Indosinian, and Yanshan-Himalayan tectonic uplifting pulses (see Fig. 2) (Zhu et al., 2009; Xu et al., 2012; Li et al., 2015). However, controlled by the tectonic framework of the basin, the intensity and time of denudation in different tectonic units varied in the same tectonism stage.

(1) Western depression

Five unconformities developed in Lower Paleozoic-Cretaceous strata in the western depression. Before the Late Triassic, the foreland basin had not yet formed in western Sichuan, and the piedmont zone and interior of the depression had the same denudation thickness. Denudation thicknesses of 500 m occurred at the end of the Middle Silurian, 200–300 m at the end of the Middle Carboniferous, and 100–200 m at the end of the Middle Triassic (Jiang et al., 2018). Since the Late Triassic, the depression had formed, and the extent of the denudation in the piedmont versus the depression differed significantly. Longmen Mountain began to uplift owing to the Yanshan Orogeny during the Late Triassic, which resulted in a period of uplift and denudation. The denudation of the piedmont zone was approximately 500–1000 m, whereas the denudation in the depression zone was smaller (approximately 100–200 m). Affected by the Himalayan Orogeny since the Late Cretaceous, northwest Sichuan suffered the most significant denudation.

Table 1
Statistical table of denudation amount in different periods of major tectonic unit(The number in parentheses is the time at which the uplift and denudation begin)

	Epoch Area	End of Middle Silurian	End of Middle Carboniferous	Early to Middle Permian	End of Middle Triassic	End of Triassic	Cretaceous to Quaternary
Western Depression	Mountain Front	500 m	200–300 m		100–200 m	500–1000 m	3200–4000 m (100 Ma)
	Interior depression	500 m	200–300 m		100–200 m	100–200 m	2000–3000 m (100 Ma)
Central Paleo-uplift	Moxi-Gaoshiti			1200-1400 (Late Silurian to Early Permian)	80–160 m		2500–3000 m (100 Ma)
	Weiyuan				80–160 m		3800–4500 m (100 Ma)
Northern Gentle Structural Zone	Northern Gentle structural zone	200 m		150–200 m		400–500 m	2500–3000 m (100 Ma)
	Daba Mountain Front	200 m					6000–7000 m (140 Ma)
Southeastern Sichuan	Eastern Fold belt	200 m		100–200 m		200–300 m	3500–4000 m (120 Ma)
	Southeastern Gentle structural zone	200 m					2000–3000 m (120 Ma)

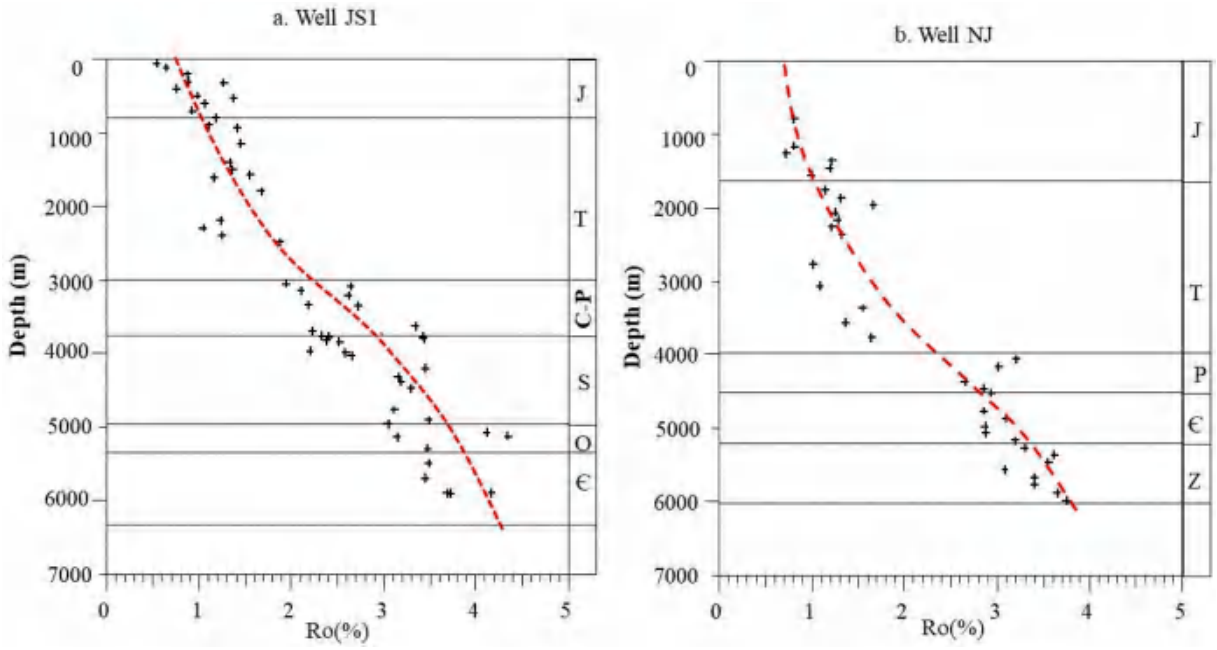

Fig. 7. The measured Ro values (Cross-shaped) and the prediction values by Easy%Ro-model (Dashed lines) of two typical wells in the Sichuan Basin.

The denudation thickness decreased from the piedmont zone (up to 4000 m) to the depression (2000–3000 m) (Jiang et al., 2018).

(2) Central Paleo-uplift

Erosional thicknesses were determined based on the trend method of stratigraphic correlation between boreholes and apatite fission track data (He et al., 2011a, b; Li et al., 2015; Mei et al., 2014; Xu et al., 2012; Deng et al., 2013). Influenced by the Caledonian Movement, the unconformity between the bottom of the Permian and the underlying strata developed continuously from the end of the Silurian to the Early Permian when the Paleo-uplift was flattened by erosion. The eroded thickness was 1200–1400 m. Affected by the uplift of the southeastern region in the Indosinian Period, the denudation height of the central Paleo-uplift was 80–160 m during the Middle-Late Triassic. The uplift amount increased gradually from the Late Cretaceous to the Neogene Period. In particular in the Neogene, the denudation extent accounted for approximately half of the total erosion. The denudation thickness of this period varied greatly within the central Paleo-uplift (2500–3000 m in the Anyue area and 3800–4500 m in the Weiyuan area).

(3) Northern gentle structural zone

The northern gentle structural zone was uplifted by the Caledonian Tectonism in the Middle and Late Silurian and exhibited a denudation thickness of approximately 200 m. Under the influenced of the Dongwu Tectonism during the Early and Middle Permian, the denudation thickness was approximately 100–200 m. The Hercynian Orogeny resulted in uplift and erosion of approximately 200–300 m in the Late Triassic. Moreover, strong uplift and denudation occurred in the Late Cretaceous in the northern Sichuan Basin owing to the Yanshanian and Himalayan orogenies with erosion of approximately 2500–3000 m. This denudation tended to increase in the southern part of the structural zone. However, the last uplift began in the Late Jurassic in front of the northern Daba Mountains, with a denudation of up to 6000–7000 m.

(4) Southeastern Sichuan Basin

This region of the basin includes an eastern steep structural zone and the southeastern gentle structural zone. Uplift and denudation with erosion of approximately 200 m occurred in the southeastern Sichuan

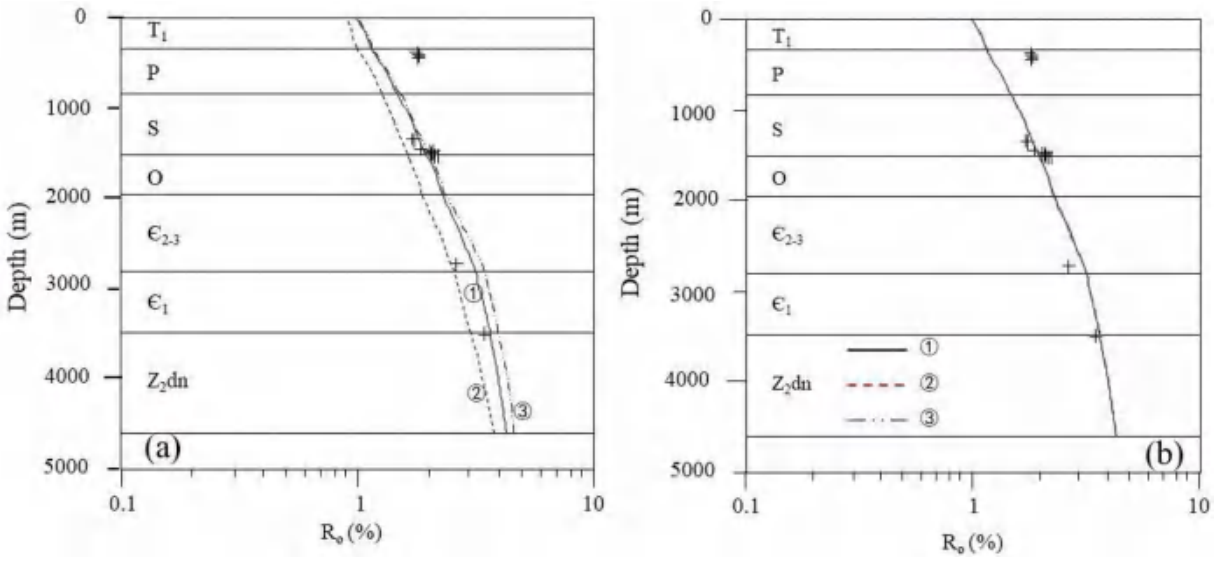

Fig. 8. Sensitivity of the Permian heat flow (a) and erosion thickness in Silurian (b) on the modeled vitrinite reflectance profiles for well DS1. The crosses are measured R_{equ} data. a. The ①, ② and ③ represent the simulation vitrinite reflectance with different Permian heat flow, ① = 72 mW/m^2 (The value used in this paper), ② = 65 mW/m^2, ③ = 90 mW/m^2 $\in_1$ = lower Cambrian; $\in_{2\text{-}3}$ = mid-upper Cambrian; O=Ordovician; S=Silurian; P=Permian; T_1 = lower Triassic. b. The ①, ② and ③ represent the simulation vitrinite reflectance with different erosion thickness, ① = 200 m (The data used in this paper), ② = 500 m, ③ = 800 m. $\in_1$ = lower Cambrian; $\in_{2\text{-}3}$ = mid-upper Cambrian; O=Ordovician; S=Silurian; P=Permian; T_1 = lower Triassic.

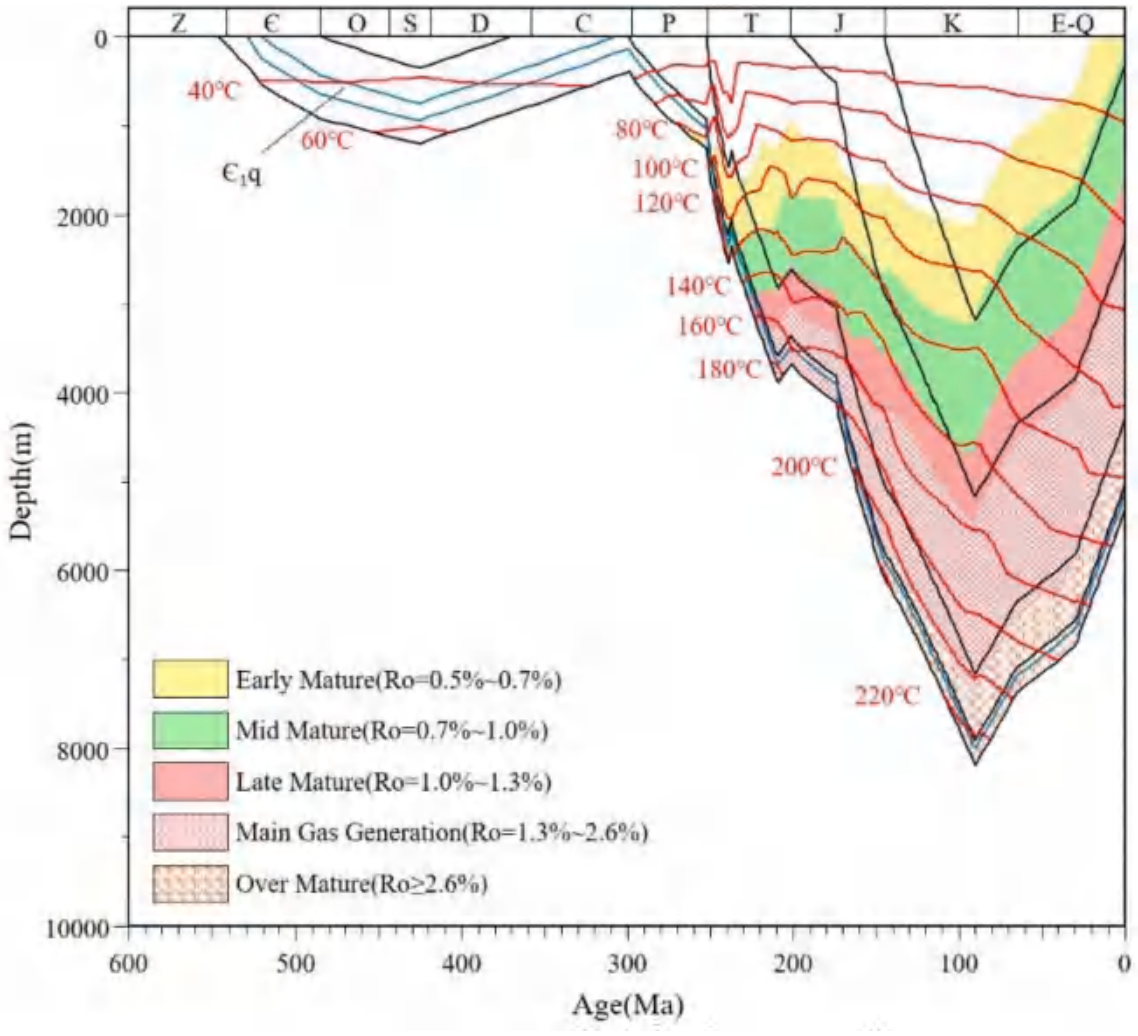

Fig. 9. The burial, thermal history and maturation of source rock in Well HS1.

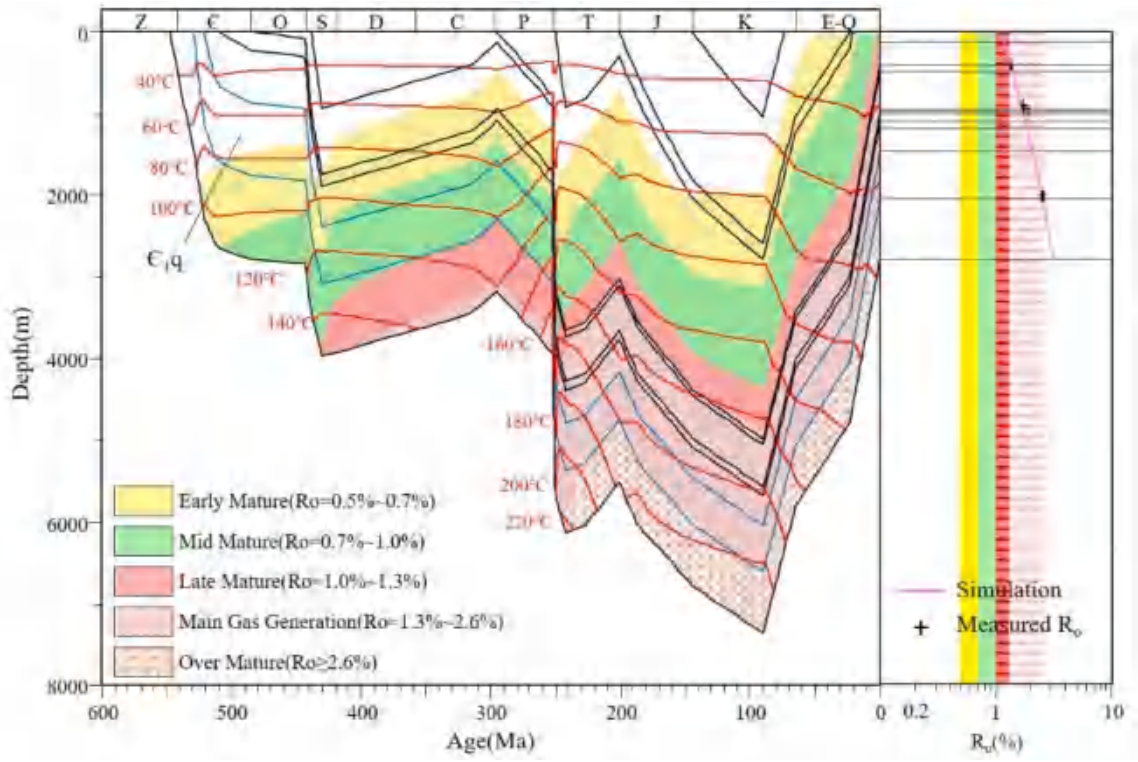

Fig. 10. The burial, thermal history and maturation of source rock in Well TX1. The right figure shows simulated and measured Ro data.

Basin during the Late Silurian. However, the strong uplift and denudation occurred under the influence of a later folding, in particular from Yanshanian-Himalayan tectonism. Subsequently, the eastern fold belts and southeastern gentle structural zone formed with denudation thicknesses of approximately 3500–4000 m and 2000–3000 m, respectively.

All uplift and denudation data noted above are listed in Table 1. In summary, the Upper Yangtze Platform is a cratonic setting, in the early stage of a stratigraphic development, and the Sichuan Basin experienced a marine deposition early in its history. The Paleo-uplift in central Sichuan was formed in the Caledonian Period, which resulted in the complete denudation of the Silurian strata with erosion of approximately 1200–1400 m. The orogenic belts were not affected by the Paleo-uplifts and experienced a low denudation during this period. However, the denudation thickness of the Yanshan-Himalayan period reached 5000–6000 m, thereby removing the entire overlying Paleozoic strata. The final uplift and denudation varied in time within the different tectonic units, with approximately 100 Ma for the western, northern, and central parts of the Sichuan Basin, 120 Ma for the eastern and southern parts of the Sichuan Basin, and 140 Ma for the Daba Mountain Front.

3.3. Kinetic model and other parameters

The kinetic model of organic matter thermal evolution is the basis of our maturity simulation. The Easy%Ro model by Sweeney and Burnham (1990) has been the most widely used model in the world. Recently, the originators have published two revised models (Basin Ro and Easy Ro-DL) to study thermal evolution. Nielsen et al. (2017) stated that the widely used Easy%Ro model overestimates vitrinite reflectance in the interval 0.45–1.7% Ro by up to 0.35%. Those authors suggested that Easy%Ro may be less accurate than Basin%Ro and Easy%RoDL, which more accurately replicates the dogleg in vitrinite reflectance versus depth in the Aurora-1 and Inigok-1 wells in Alaska at depths corresponding to ~0.7–1.0% Ro (Peters et al., 2018). Replication of the dogleg and simultaneous calibration of the two segments was not possible with Easy%Ro.

The Ro values predicted by different models are quite different at higher maturity (e.g., Ro>1.7%). For example, the basin%Ro-model Ro value is 4.5%, but the Easy%R-model Ro value is only 3.5% at temperature 250 °C (Nielsen et al., 2017). The basin%Ro-model shows a second section of higher gradient linear increase at high temperature (Suggate, 1998; Nielsen et al., 2017). At the same time, the difference between the basin%Ro-model and Easy%R-model Ro values is only reflected below the depth of 4000 m in wells Aurora-1 and Inigok-1 (Peters et al., 2018). The dogleg Ro profiles of these two wells maybe imply that the deep strata experienced different thermal history from that of the shallow strata. However, such dogleg Ro profile does not exist in Sichuan Basin, and most Ro profiles are linear. The Easy%Ro-model Ro value fit well with the measured data and can be used to predict Ro values in the deep strata (Fig. 7). So we applied the widely used Easy%Ro model to calculate maturity of resource rocks with the BasinMod software provided by Platte River Associates (PRA) Inc.

Isopach maps for all strata were provided by the Southwest Oil and Gas Field Branch, CNPC, and paleo-heat flow and erosion data are based on our new data described above. In our modeling, the fluid flow model of compaction method is applied (Sclater and Christie, 1980; Bethke, 1985). The thermophysical parameters of the rocks are taken from Zhu et al. (2015, 2017). The surface temperature of the whole geological history was set at 20 °C, and most important, paleothermal indicators of vitrinite reflectance, bitumen reflectance (e.g. R_{equ}), and some apatite fission track data were used to calibrate our thermal models. In our study, the thermal indicator data were also a key factor in the thermal history reconstruction. However, measurement errors may reduce the reliability of the modeled results. Errors in the apatite fission track data used in our model were generally less than ±3%, and the errors in the R_{equ} data were smaller than ±10% (Qiu et al., 2012).We concur with Li et al. (2010) that the accuracy of the thermal modeling results using R_{equ} data is approximately ±5%.

Heat flow and erosion thickness are key parameters of maturity simulation. Here, we discuss the sensitivity of Permian heat flow and erosion thickness at the end of middle Silurian on the modeled vitrinite

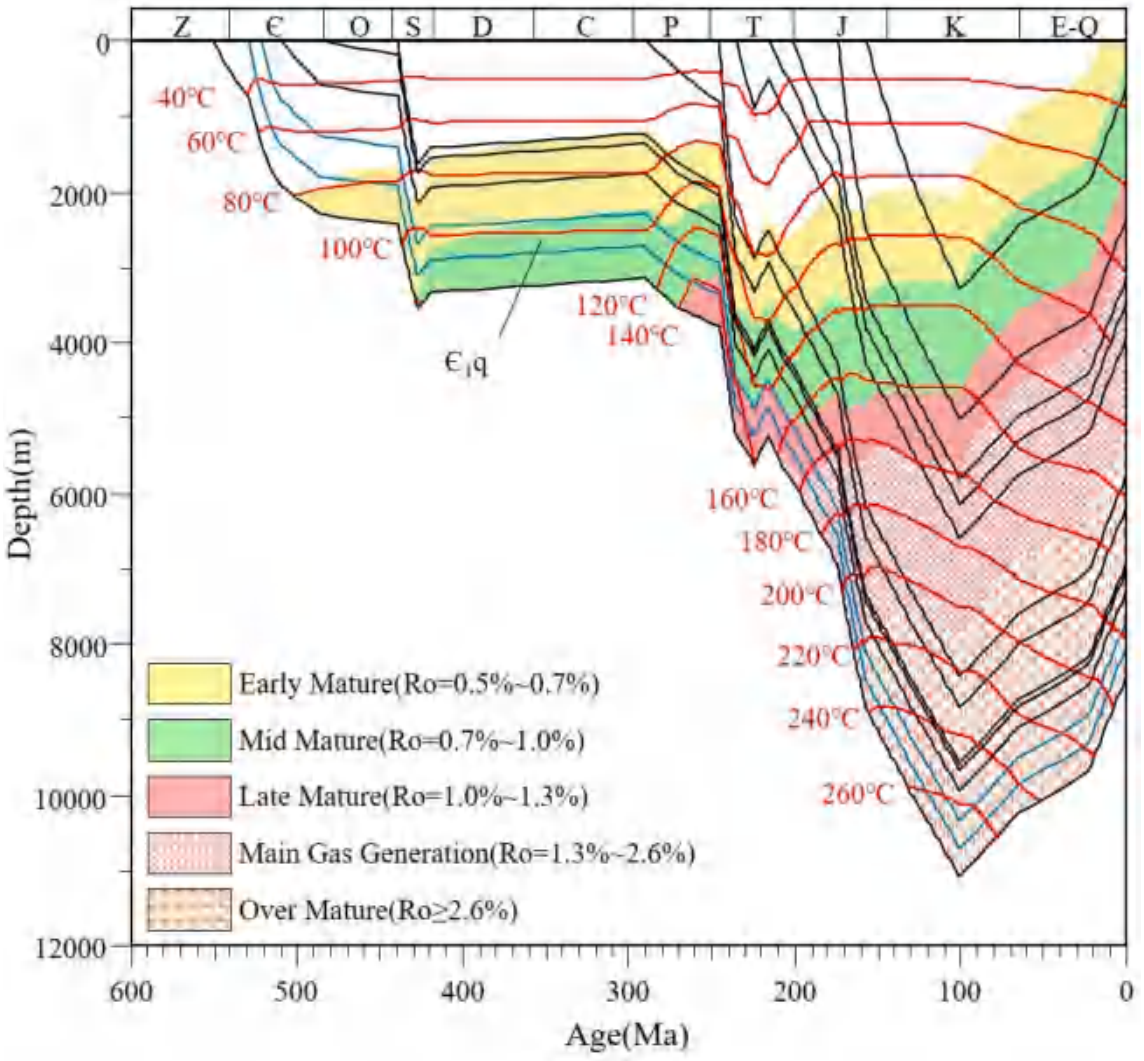

Fig. 11. The burial, thermal history and maturation of source rock in Well MS1.

reflectance (R_o) profiles. As discussed above, heat flow values for the Permian are quite variable across the different tectonic units. Since the maturity of source rocks had mostly reached the maximum values before the uplift associated with Yanshan tectonism, we only discuss the influence of Silurian denudation. Thermal maturity profiles and the maturity history of Cambrian source rocks in well DS1 for different Permian thermal scenarios were modeled (Fig. 7a). Thermal maturity profiles were calculated by assuming the different Permian heat flow of the best-case result (e.g., well DS1 in Fig. 8a). When the heat flow value was changed to be 65 mW/m^2, the R_{equ} profile appeared to be inconsistent with the measured values in the upper Paleozoic section. When the heat flow was adjusted to be 90 mW/m^2, the R_{equ} profiles in the Cambrian remained inconsistent with the measured R_{equ} data. When the heat flow was adjusted to 72 mW/m^2, the value adopted in the present study, R_{equ} profiles were consistent with the measured R_{equ} data. In addition, thermal maturity profiles of well DS1 were also calculated by assuming different erosion amounts in Silurian (Fig. 8b). We changed the erosion amount from 200 m to 800 m, the R_{equ} profiles were consistent with the measured R_{equ} data. This demonstrates that the amount of Silurian denudation has no effect on the final maturity.

4. Maturity evolution of Lower Cambrian

The source rock maturity evolutions of typical wells (Fig. 1) were calculated, and the evolution patterns of the source rocks were obtained based on the simulation results for these typical wells in five tectonic units. Moreover, the equivalent vitrinite reflectance (R_{equ}) was used to present the maturity of the source rocks. The maturity history was classified as follows:

Early mature, 0.5 %< Requ <0.7 %
Middle mature, 0.7 %< Requ <1.0 %
Late mature, 1.0 %< Requ <1.3 %
High mature, 1.3 %< Requ <2.6 %
Over mature, Ro>2.6%

4.1. Thermal maturity evolution of typical wells

4.1.1. Wells HS1 and TX1 in the western depression

Well HS1 is located in the south part of the depression, which lacks Ordovician- Carboniferous strata. The Lower Cambrian Qiongzhusi Formation source rocks began to evolve with the increase in burial depth in the Early Paleozoic. However, the maturity was only approximately 0.4% (immature) of the equivalent vitrinite reflectance (R_{equ}). Subsequently, the evolution of the source rocks halted temporarily owing to an uplift caused by the Caledonian Tectonism. Since the Early Permian, the strata became deeply buried again, and the temperature increased

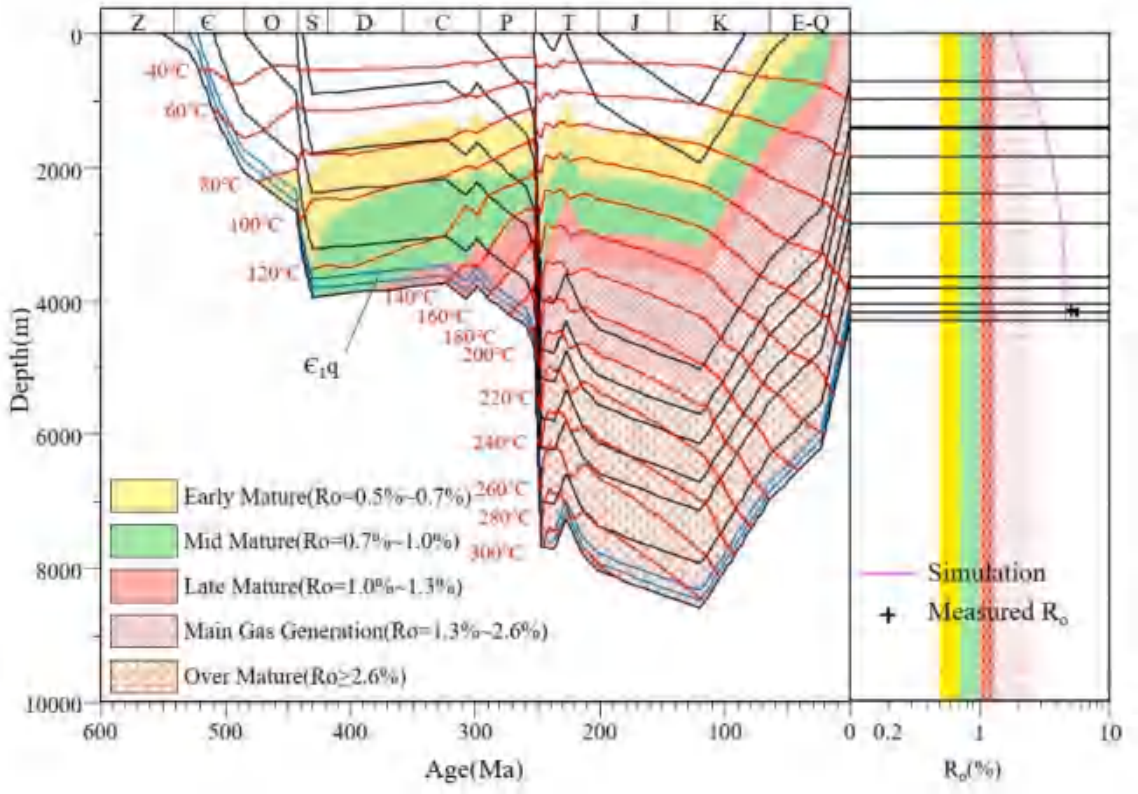

Fig. 12. The burial, thermal history and maturation of source rock in Well JS1.

rapidly. From the beginning of the Triassic period, the source rocks experienced a period of rapid maturation. The source rocks began to mature in the Early Triassic and entered the high-mature stage by the Late Triassic (R_{equ}>1.3%). By the end of the Jurassic, the source rocks were over-mature (R_{equ}>2.6%). During the Middle and Late Cretaceous, the degree of thermal evolution of the source rocks reached the highest level. Subsequently, maturation ceased as the strata began to uplift and the temperatures decreased (Fig. 9).

Well TX1 is located in the north part of the depression. The Lower Cambrian Qiongzhusi Formation source rocks entered the hydrocarbon generation threshold in the Late Cambrian and reached the mid-mature stage in the Middle and Late Silurian (R_{equ} > 0.7%). Subsequently, maturation ceased as the strata began to uplift and the temperatures decreased. In the Middle and Late Permian, the maturity began to increase rapidly owing to the influence of the increasing heat flow and progressive burial. Consequently, the Qiongzhusi Formation source rocks entered the main gas generation stage (Fig. 10).

4.1.2. Well MS1 in the northern structural zone

The Lower Cambrian Qiongzhusi Formation source rocks in Well MS1 began to mature in the Ordovician. Subsequently, the thermal evolution decreased owing to the uplift during the Caledonian Movement. From the beginning of the Middle and Late Triassic periods, the source rocks experienced a period of rapid evolution and entered the late-mature stage. The strata entered the main gas generation stage in the Jurassic, due to continuous burial and a rapidly increasing temperature. Source rock maturity reached the highest level in the Middle and Late Cretaceous periods. Subsequently, it ceased to evolve owing to an uplift of the strata and decrease in the temperature (Fig. 11).

4.1.3. Wells JS1 and WT1 in the eastern structural zone

The Lower Cambrian Qiongzhusi Formation in Well JS1 gradually matured in the Early Paleozoic and entered the early-mature stage (R_{equ}>0.5%) in the Middle and Late Ordovician. With increasing burial depth, the maturity exceeded 0.7%R_{equ}. During the Early Carboniferous, the source rock entered the late-mature stage. However, it experienced rapid burial from the Early to Middle Triassic and reached the over-mature stage directly. Thereafter, the formation temperature began to decrease, and the maturation did not progress further (Fig. 12).

The Lower Cambrian Qiongzhusi Formation in Well WT1 matured rapidly in the Early Paleozoic and entered the early-mature stage (R_{equ} = 0.5%) in the Late Ordovician. Moreover, a rapid-maturation period occurred in the Middle and Late Permian, reaching the high-mature stage with R_{equ}>1.3%. Although the thermal evolution experienced a temporary stagnation in the Triassic, the maturity increased rapidly afterward and reached the highest level in the Middle and Late Cretaceous. Subsequently, the formation temperature decreased owing to tectonic uplift, and thermal evolution ceased (Fig. 13).

4.1.4. Wells DS1 and N2 in the southern structural zone

The total thickness of the Lower Paleozoic strata exceeds 2500 m in the southern Sichuan Basin. This deep burial and heating caused the source rocks of the Qiongzhusi Formation in Well DS1 to reach the oil generation threshold in the Ordovician, peak oil generation in the Middle Silurian, and a high-mature stage at the end of the Middle Silurian. Thereafter, the strata began to uplift slowly, and the thermal evolution of the source rocks of the Qiongzhusi Formation was greatly reduced. Another rapid evolution of the source rocks occurred in the Early Permian, and the over-mature stage was reached in the Early Jurassic. The thermal evolution ceased gradually after the Middle and Late Cretaceous (Fig. 14).

The Lower Cambrian source rocks of the Qiongzhusi Formation in Well N2 began to mature in the Middle and Late Cambrian (R_{equ} = 0.5–0.7%), and reached the middle-mature stage in the Late Ordovician (R_{equ} = 0.7–1.0%). After the Middle Silurian, the thermal evolution of the source rocks stagnated owing to uplifting and cooling. Again, the maturation rapidly increased in the Middle and Late Permian owing to an increasing heat flow. After the Late Cretaceous, the maturity

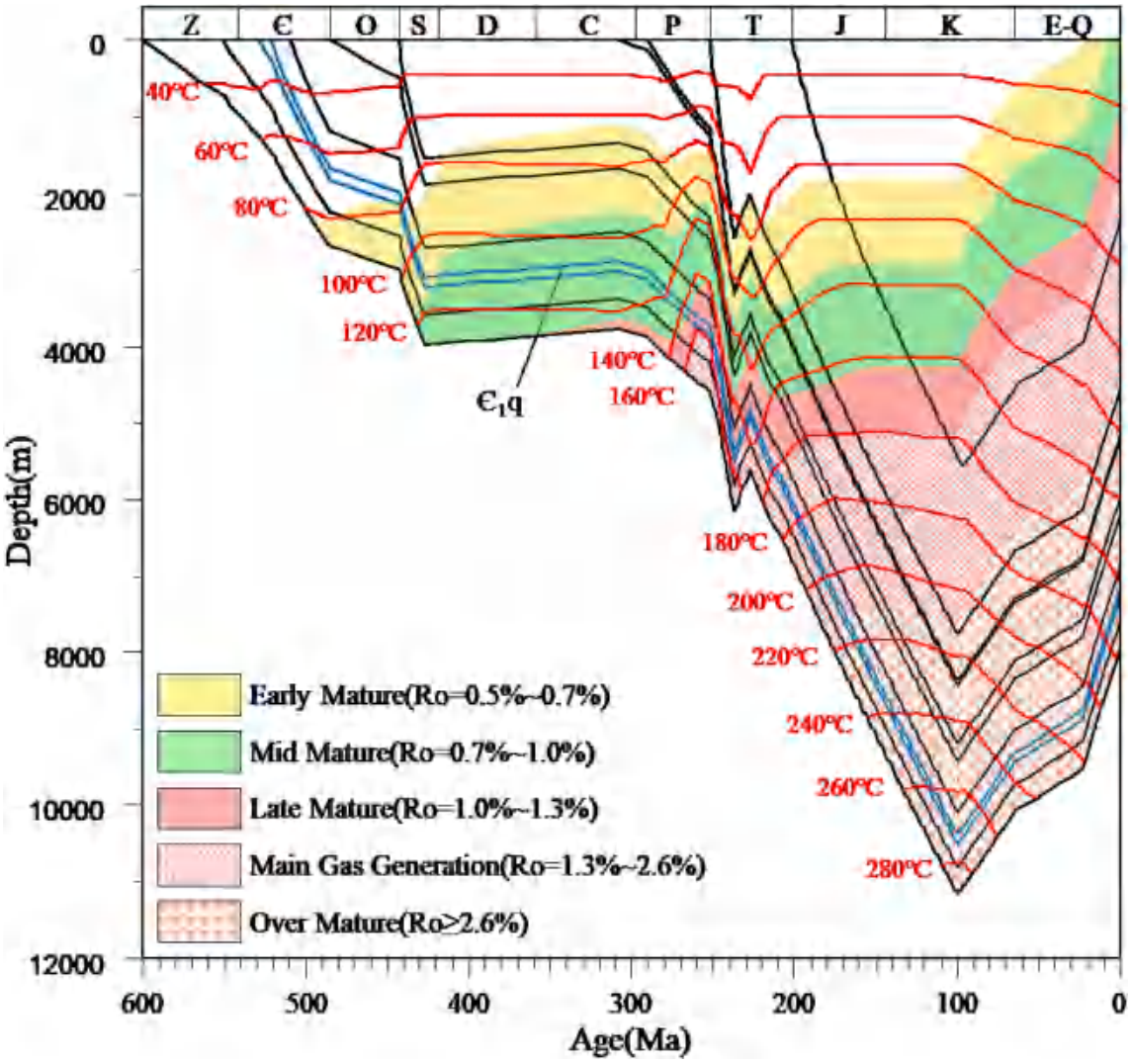

Fig. 13. The burial, thermal history and maturation of source rock in Well WT1.

remained unchanged owing to tectonic uplift (Fig. 15).

4.1.5. *Wells GS1and CS1 in the central Paleo-uplift*

The Lower Cambrian source rocks of the Qiongzhusi Formation in Well GS1 began to enter the early-mature stage at the end of the Middle Silurian. With the Caledonian orogeny, the central Sichuan region began to uplift, which resulted in the suspension of the thermal evolution of the source rocks from the Devonian to the Early Permian period. The source rocks of the Qiongzhusi Formation experienced a rapid evolution in the Middle and Late Permian and entered the mid-mature stage. Subsequently, the thermal evolution of the source rocks was suspended again during the Triassic. Since the Early Jurassic, the source rocks of the Qiongzhusi Formation matured rapidly owing to increasing burial and temperature. They reached the maximal maturity (R_{equ} > 2.6%). Thereafter, with the uplift of the basin, the formation temperature decreased and the source rocks ceased to evolve (Fig. 16).

The thermal evolution process of source rocks of the Qiongzhusi Formation in Well CS1 is different from that of Well GS1. The Qiongzhusi Formation entered an early-mature stage in the Early Silurian and reached mid-mature stage by the end of the Silurian. With the Caledonian tectonism and strata uplift, the thermal evolution from the Devonian to the Early Permian was suspended. Since the Middle and Late Permian, the source rocks of the Qiongzhusi Formation experienced a rapid evolution and reached the over-mature stage in the Middle Jurassic. After the Late Cretaceous, the source rocks ceased to evolve owing to tectonic uplift (Fig. 17).

4.2. *Evolution pattern of the Qiongzhusi Formation source rock*

The thermal evolution pattern of the Qiongzhusi Formation source rocks in the Sichuan Basin can be classified into three types based on a comprehensive analysis of the thermal evolution process and maturity stages of typical wells: (1) Continuous heating pattern, where the source rocks have been continuously heated and undergone maturation since deposition. (2) Silurian-Permian heating cessation pattern. The source rocks experienced a pause in heating and maturity stagnation during the Silurian and Permian. (3) Silurian-Permian and Triassic heating cessation patterns. The source rocks experienced two pauses in heating and maturation at the Silurian-Permian and Triassic, respectively.

4.2.1. *Continuous heating pattern*

This pattern mainly exists in the Southern Sichuan Basin. The thermal evolution of the source rocks was relatively continuous and matured early after deposition and compaction. Hydrocarbon generation began in the Early Paleozoic, and the maturity continued to increase. Although the heating was variable, no prolonged periods of heating cessation occurred during this period. The thermal evolution stopped gradually after the Mesozoic, and the hydrocarbon source rocks entered an over-

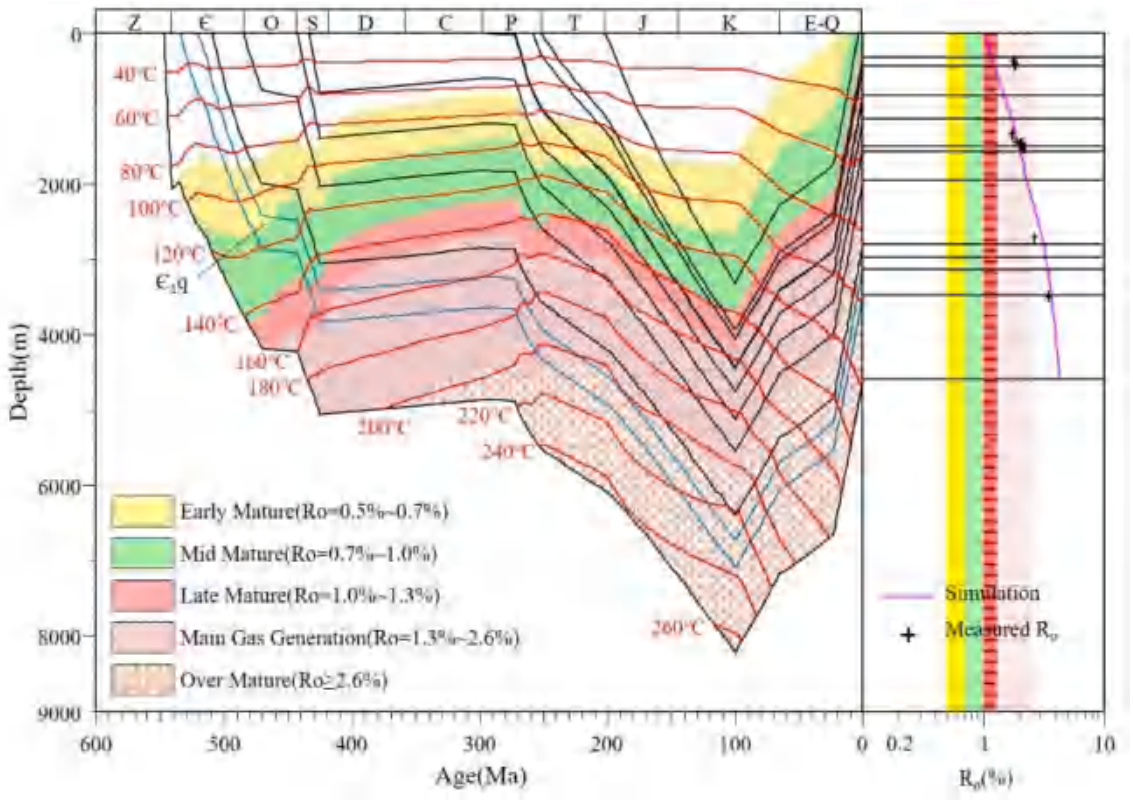

Fig. 14. The burial, thermal history and maturation of source rock in Well DS1. The right figure shows simulated and measured Ro data.

mature stage (Fig. 18).

4.2.2. Silurian-Permian heating cessation pattern

This pattern mainly occurs in the western depression and northwestern central Paleo-uplift. The main feature is the significant heating stagnation from the Early Silurian to the Late Permian period (Fig. 19). Thermal evolution of the source rock included four stages, ① early variable heating in the Early Paleozoic, when the maturity level of the Lower Cambrian source rocks increased slowly, and remained at the immature to early-mature stage, ② long limited heating stage during the Late Silurian and Late Permian, owing to tectonic uplift and a decrease in formation temperature, ③ late variable heating from the Late Permian to Jurassic, when the source rocks matured rapidly. ④ steady-state heating from the Cretaceous to present, where the thermal evolution stopped gradually, and the maturity level did not increase further.

4.2.3. Silurian-Permian and Triassic heating cessation pattern

This pattern mainly occurs in the central Paleo-uplift, northern structural zone and western part of the eastern structural zone. The main feature is two significant heating pauses at the Silurian-Permian and Triassic (Fig. 20). Thermal evolution of the source rock included five stages: ① early variable heating in the Early Paleozoic, as the maturity level of the Lower Cambrian source rocks increased slowly, and remained at an early-mature stage, ② long limited heating during the Devonian and Late Permian, owing to tectonic uplift and a decrease in the formation temperature, ③ late variable heating in the Early Triassic, with a short period of rapid-maturation, ④ short-time limited heating during the Middle to Late Triassic, and ⑤ steady-state heating from Jurassic to present, when the source rocks experienced the second rapid-maturation stage. Furthermore, the thermal evolution ceased gradually, and the maturity did not increase after the Middle and Late Cretaceous.

5. Discussion

5.1. Key periods of hydrocarbon generation in Qiongzhusi Formation of different tectonic zones

Owing to the different thermal evolution patterns of the Qiongzhusi Formation ($Є_1q$), the key stages of hydrocarbon generation are obviously different in five structural units of the Sichuan Basin (Fig. 21). At the end of the Silurian, the distribution of the matured $Є_1q$ source rock within the basin was arc-shaped around the Caledonian uplift, that is, the $Є_1q$ did not enter the hydrocarbon generation threshold in western Sichuan, whereas it entered peak oil generation ($R_{equ} = 0.8–1.3\%$) in the eastern and southern Sichuan. In the Late Permian, the period of the Emeishan mantle plume activity, the thermal evolution of $Є_1q$ reached a new stage after the stagnation in the Devonian and acceleration in the Early Permian. Southwest Sichuan is located in the intermediate zone of the Emeishan large igneous province (He et al., 2003), in which the hydrocarbon source rocks of $Є_1q$ evolved rapidly into hydrocarbon generation owing to the substantial burial and intense heating; R_{equ} exceeded 1.6% (2.6% locally) at approximately 252 Ma. In other areas, constrained by the distance from the center of the Emeishan mantle plume activity, the heating effect was not as strong as that of southwest Sichuan. However, the effect of the high heat flow on the maturity evolution of Cambrian source rocks cannot be neglected. At the end of the Permian, except for the Mianzhu in northwest Sichuan and Weiyuan-Nanchong in the central uplift, the Qiongzhusi Formation entered the oil-cracking to gas generation stage, and even the dry gas stage ($R_{equ} > 2.6\%$) at the edge of the eastern Sichuan Basin. After the Indosinian Tectonism, the maturity distribution of $Є_1q$ changed with the formation of Longmen Mountain.

At the end of the Triassic, the Qiongzhusi Formation in the western Sichuan piedmont and the present central uplift were in the late-mature stage, while other parts of the Sichuan Basin entered the over-mature stage, (R_{equ} of the Qiongzhusi Formation in northern Sichuan was

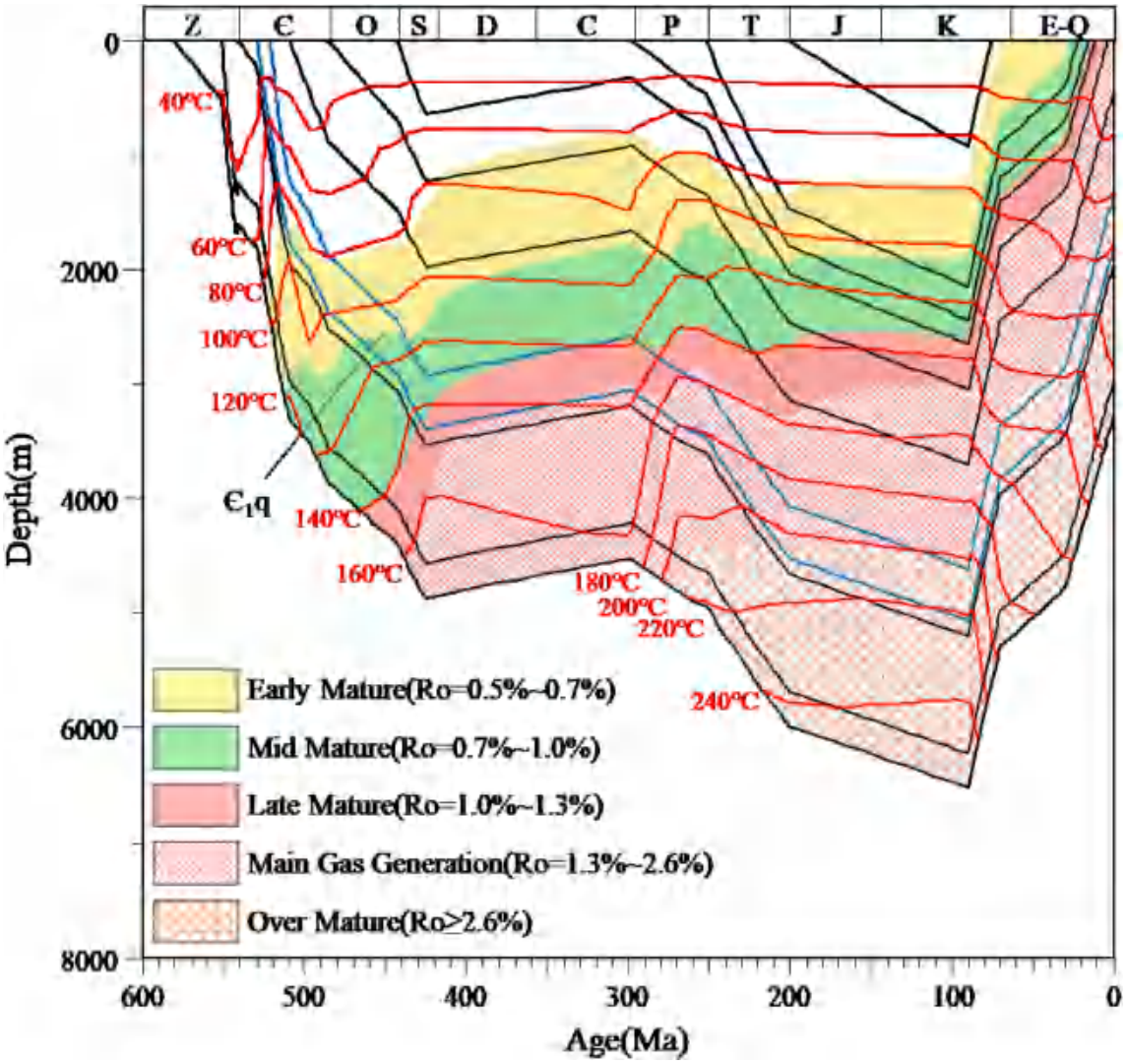

Fig. 15. The burial, thermal history and maturation of source rock in Well N2.

1.2–1.8%, 1.6–3.8% in eastern Sichuan, and even 3.0–4.0% in southern Sichuan). By the end of the Jurassic, all Qiongzhusi hydrocarbon source rocks had reached the over-mature stage in the Sichuan Basin and the distribution pattern remained basically equal. Except for the Mianyang area in northwestern Sichuan and the northern part of the central uplift, R_{equ} exceeded 3.0% in all other areas. Before the final stage of uplift, the maturation continued during the Early Cretaceous, and the Qiongzhusi Formation reached maximal thermal maturity at the end of the Early Cretaceous, thereby forming the extant maturity distribution pattern. The two maturity centers formed at the end of the Jurassic period in the western Sichuan depression and eastern Sichuan connected to form a northwest–southeast zone of high maturity; R_{equ} exceeded 4.0%, and R_{equ} in southern Sichuan approached the hydrocarbon generation limit of 4.5%. In all areas except for the Weiyuan-Ziyang region of the central uplift and the front-zone of the Longmen Mountain, the equivalent vitrinite reflectance of the Qiongzhusi Formation of the Sichuan Basin was above 4.0%.

5.2. Influences of Paleozoic tectonic movements on thermal evolution model of Qiongzhusi Formation

Based on the reconstruction of burial history and thermal evolution of the Qiongzhusi Formation in different structural units, it was believed that the present maturity of the Qiongzhusi Formation is mainly controlled by the continuous subsidence since the Triassic. However, the maturity evolution pattern affecting the key hydrocarbon generation stage was mainly related to the tectonic movements in the Paleozoic marine sedimentation stage.

The current formation thickness of the Cambrian was generally thick in the Southeast and thin in the Northwest. Although the thickness of the Ordovician was smaller than that of the Cambrian, the increase in the thickness was consistent with that of the Cambrian. Hence, from the Cambrian to the Ordovician, subsidence in the southeastern Sichuan Basin was relatively large, thereby leading to a more rapid thermal evolution of the Qiongzhusi Formation. Furthermore, the hydrocarbon source rocks in the southeastern area entered the hydrocarbon generation threshold and oil generation peak at the earliest, which is consistent with previously thermal evolution results (Rao et al., 2013; Zhu et al., 2010; Zou et al., 2014a).

During the Caledonian Tectonism since the end of the Silurian, the collision and subduction between the Pacific plate and Eurasian plate caused a large uplifting area in the middle Yangtze Plate, thereby resulting in the formation of the central Paleo-uplift in the Sichuan Basin. At this time, the Ordovician-Silurian strata suffered intense erosion (Liu et al., 2012, 2016). Owing to the continuous uplift in the Devonian, Devonian strata are widely absent in the basin. After a short period of Carboniferous deposition, the Dongwu Tectonism beginning in the Late Carboniferous caused the basin to be uplifted again and

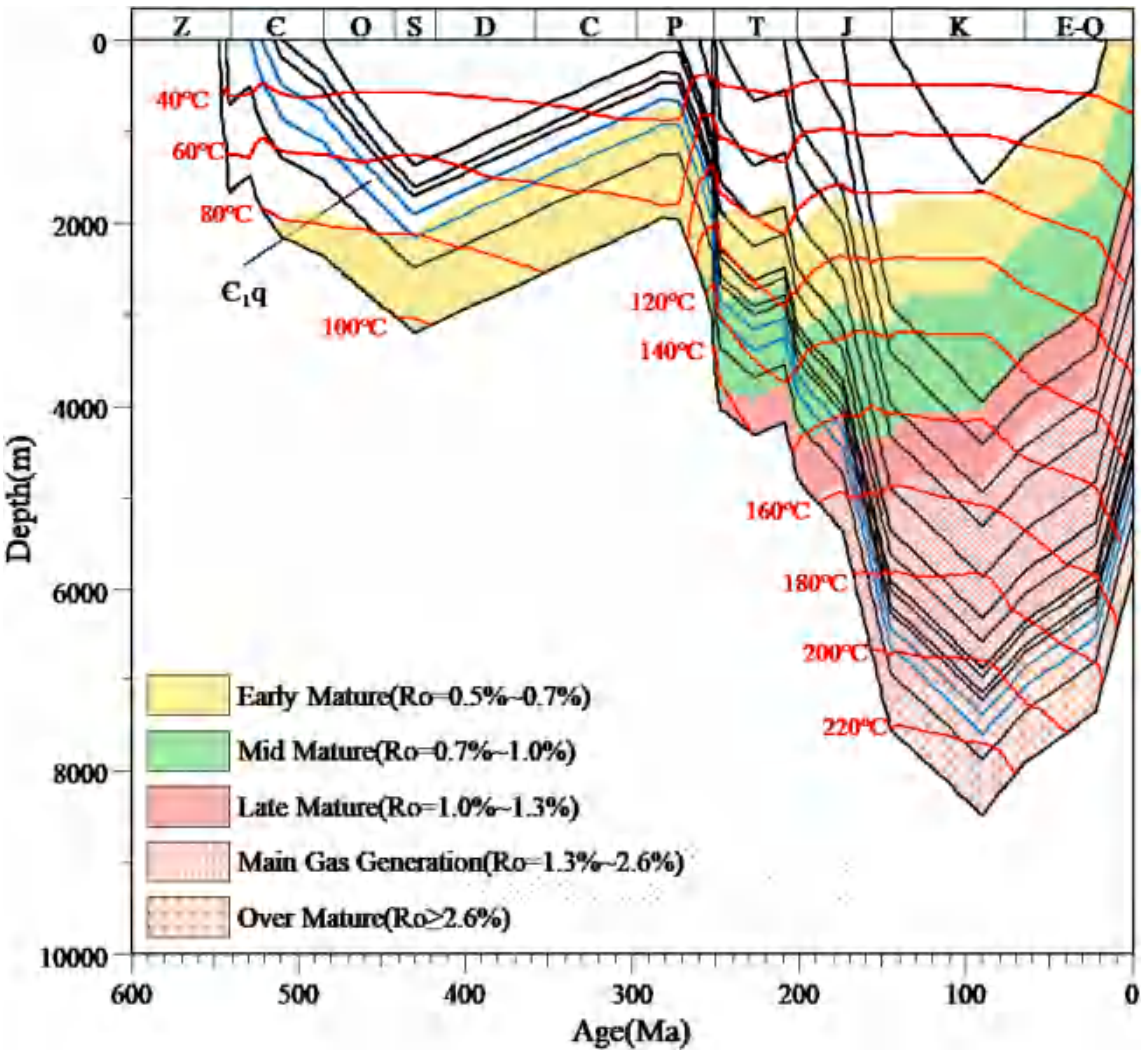

Fig. 16. The burial, thermal history and maturation of source rock in Well GS1.

experienced denudation. Few Carboniferous sedimentary deposits remain in the northeast of the basin. As a result, the uplift and denudation from the end of the Silurian to the Early Permian (Caledonian Movement) halted maturation of hydrocarbon source rocks in the Qiongzhusi Formation for a long period, thereby leading to the platform pattern of the thermal evolution in most parts of the basin. However, the Caledonian Movement had little effect on the southeastern margin, which experienced significant subsidence in the early stage. Since the Permian, the Yangtze Plate subsided as a whole, and in particular the large-scale transgression in the Middle Permian caused the Yangtze area to become a carbonate platform. Consequently, the calcareous shale of the Qiongzhusi Formation experienced a rapid-mature stage. So far, the tectonic activities in Sichuan Basin are mainly uplift and subsidence. Thus, the thermal background of the Qiongzhusi Formation was controlled by a single factor in the basin, and no abnormal thermal events changed the maturation of the strata. However, the eruption of the Emeishan basalt in the Late Permian changed the thermal state of the surrounding strata, which accelerated the maturation of the Qiongzhusi Formation in the Southwest and that of the central uplift of the Sichuan Basin in the Late Permian. For example, compared with the north, the southern edge of the western Sichuan depression reached the hydrocarbon generation threshold and peak oil generation later and the gas generation stage earlier (Fig. 21). The diameter of the Emeishan mantle plume head was 1600–1800 km (Jiang et al., 2018). Since the center of Sichuan Basin is about 1000 km northwest of the center of Emeishan mantle plume, we speculate that the thermal effect of mantle plume decreases towards the northeast of Sichuan Basin. In fact, thermal indicators of vitrinite reflectance can record the effect of mantle plume, and we only found a thermal effect in the vitrinite reflectance in the southern and central part of the basin (Jiang et al., 2015; Zhu et al., 2010, 2016, 2017, 2018). Hence, except for local regions far away from the Emeishan mantle plume (e.g. the north and northeast of the Sichuan Basin), the heat effect of the mantle plume altered the thermal histories of most parts of the Sichuan Basin (Liu et al., 2018).

Therefore, tectonic and sedimentary burial and the eruption of Emeishan basalt in the Late Permian were the main factors controlling the thermal evolution models of the Qiongzhusi Formation. Regarding the hydrocarbon source rocks of the Qiongzhusi Formation, the basement tilt to the Southeast due to the supercontinent breakup caused the southeastern Sichuan Basin to reach the hydrocarbon generation threshold and peak oil generation earliest; the uplift and denudation during the Caledonian and Dongwu Movements delayed the thermal evolution in the entire basin. Moreover, the Emeishan volcanic activity changed the thermal constitution of some parts of the basin, thereby accelerating thermal evolution in the Southwest and central Sichuan Basin.

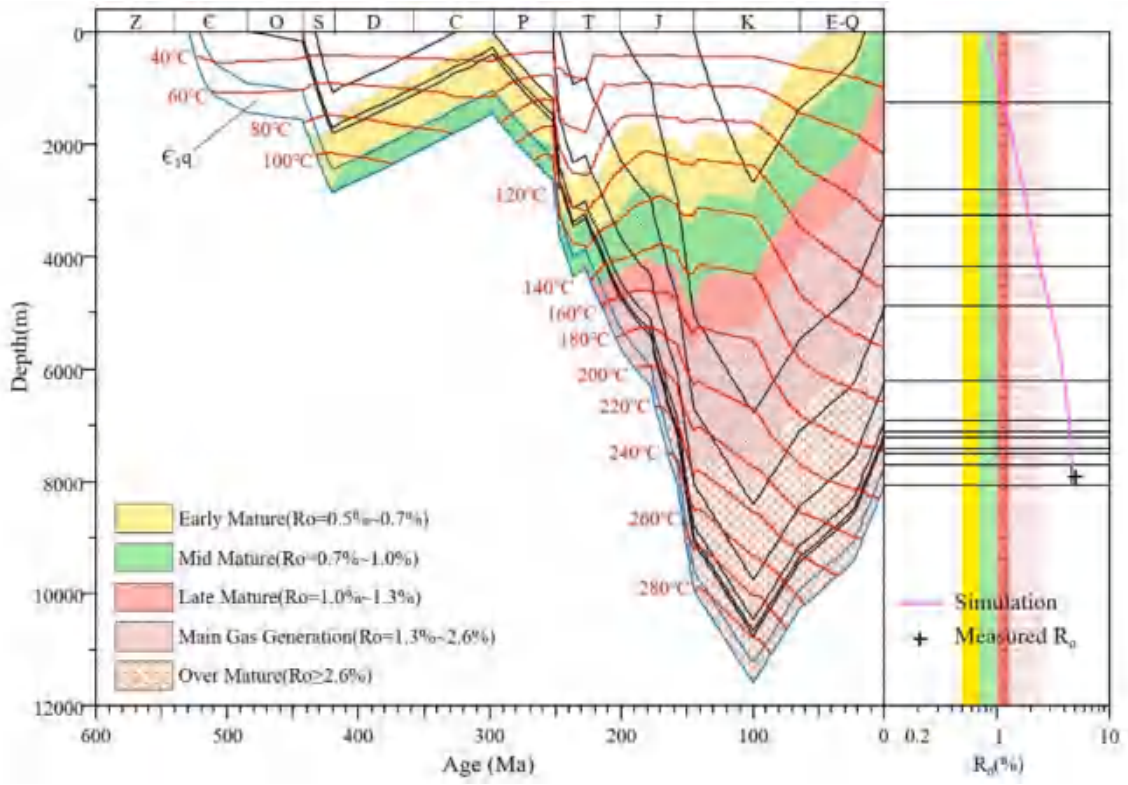

Fig. 17. The burial, thermal history and maturation of source rock in Well CS1. The right figure shows simulated and measured Ro data.

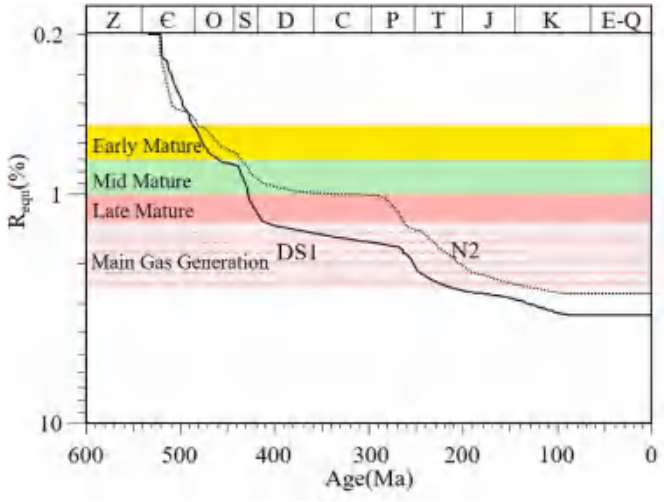

Fig. 18. Continuous heating pattern of the Qiongzhusi Formation source rock.

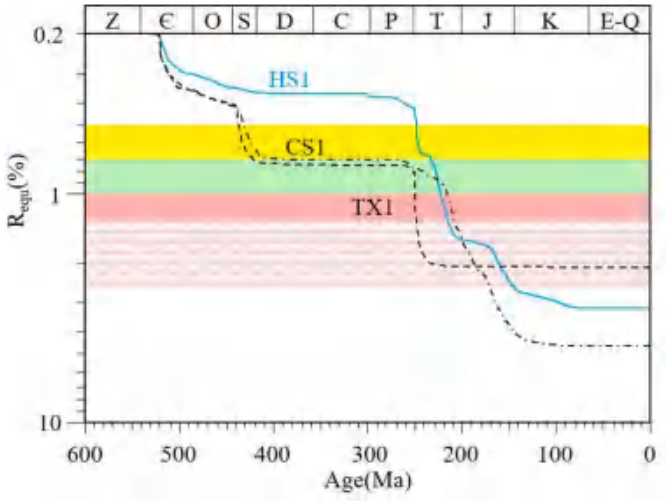

Fig. 19. Silurian-Permian heating cessation pattern of the Qiongzhusi Formation source rock.

5.3. Effects of Mesozoic sedimentation on the present maturity of the Qiongzhusi Formation

After the Emeishan Movement, the Sichuan Basin entered a continuous subsidence stage again, and the upper Yangtze Plate basically exhibited the Late Permian tectonic pattern in the Early Triassic (e.g., the overall structure was higher in the West and lower in the East). Because the Qinling Ocean between the Yangtze Plate and North China Plate expanded from the east to the west, the Sichuan Basin was uplifted in the Middle Triassic, and the seawater gradually withdrew from the Yangtze Plate to the west. Consequently, the basin turned into a continental sedimentary environment. The Middle Triassic Leikoupo formation experienced erosion up to 160 m in the eastern and central parts of the basin. However, controlled by the structural pattern, the effects of the denudation on the thermal evolution of the Qiongzhusi Formation were different. For example, owing to the separation of the aulacogen in the central Sichuan area, Well GS1, located in the gentle slope zone on the right side of the aulacogen, experienced a short stagnation of its thermal evolution in the Early-Middle Triassic. It began to mature rapidly at the end of the Triassic. However, wells ZY1 and Z4, located in the aulacogen, were not affected by uplift and denudation during the Middle Triassic, which lead to rapid maturation starting at the end of the Permian (Fig. 22).

By the end of the Late Triassic, the Longmen Mountain thrust belt formed during the Paleo-Tethys Ocean closure, and the western Sichuan

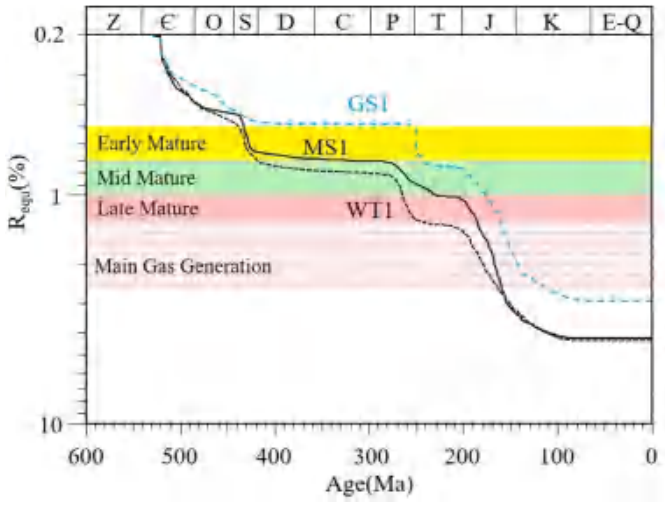

Fig. 20. Silurian-Permian and Triassic heating cessation pattern of the Qiongzhusi Formation source rock.

area changed from a passive continental margin to a foreland basin. From the Jurassic to the Early Cretaceous, the Sichuan Basin became a large intracontinental depression basin with the formation of a thrust zone around the basin. The Mesozoic strata were relatively thin in eastern Sichuan and generally thick in central and western Sichuan. This period was the main stage of the thermal evolution of the central and western Sichuan Basin, the maturity of the Qiongzhusi Formation reached a maximum, thereby forming the present maturity distribution pattern. In the Early Cretaceous period, the western Hunan-Hubei tectonic belt in the eastern margin of the Sichuan Basin began to uplift and was gradually transferred toward the basin. Furthermore, the depocenter of the basin tended to migrate to the front of the Longmen Mountain. Influenced by the Yanshanian and Himalayan Movements, from the Late Cretaceous to the Cenozoic, the Sichuan Basin experienced rapid uplift (up to 4000–5000 m), and most Cretaceous and Jurassic strata were denuded. Therefore, the present-day formation thickness of the Mesozoic strata and the denudation of the last stage directly affected the present maturity of hydrocarbon source rocks of the Qiongzhusi Formation.

6. Conclusions

In this study, the maturity histories of the effective source rocks in the Sichuan Basin (Lower Cambrian strata) were modeled with the kinetic model Easy%Ro and newly obtained thermal history and erosion amounts with the BasinMod software provided by Platte River Associates Inc. Maturation of Qiongzhusi Formation source rock in 9 typical wells from different tectonic units were modeled, based on the new thermal history and denudation data. Three maturity evolution patterns of the Qiongzhusi Formation source rock in the Sichuan Basin were classified, which are continuous heating pattern, Silurian-Permian heating cessation pattern and Silurian-Permian & Triassic heating cessation. The key hydrocarbon generation periods of different structural units were also obtained. The eastern and southwestern-southern Sichuan were the early hydrocarbon generation centers with the Qiongzhusi Formation entering the threshold of hydrocarbon generation earliest, with peak oil generation occurring at the end of the Silurian and the dry gas generation stage at the end of the Permian. Owing to the thermal effect of the Emeishan mantle plume, the hydrocarbon source rocks of the Qiongzhusi Formation in the south of western Sichuan depressions entered the peak oil generation later than that in the north, but

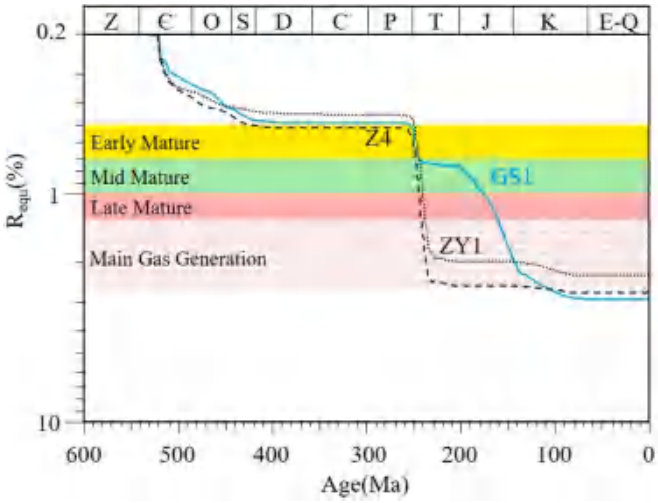

Fig. 22. Comparison of thermal evolution of the Qiongzhusi formation between the gentle belt (GS1) and aulacogen (ZY1, Z4) of central paleo-uplift.

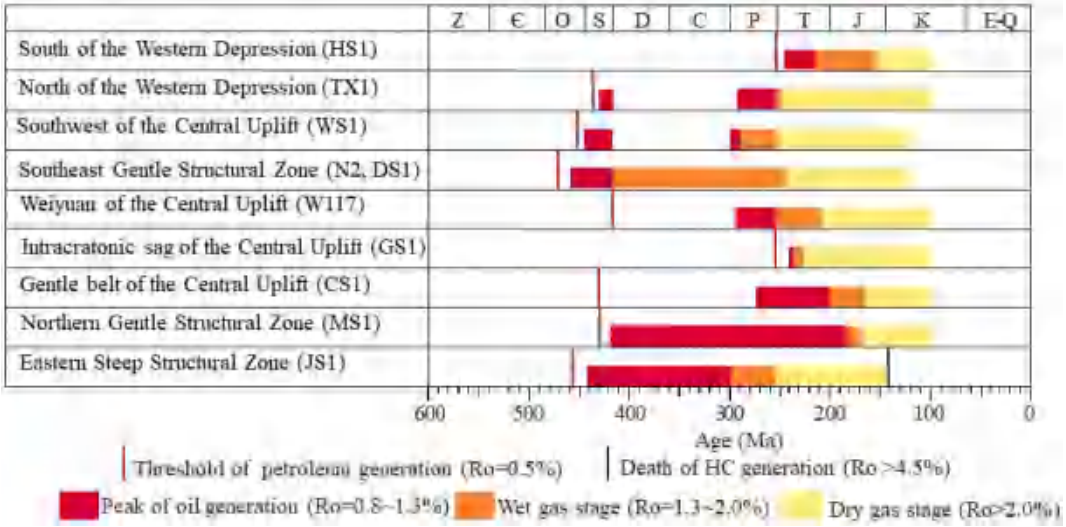

Fig. 21. Critical period of thermal evolution of the Qiongzhusi Formation source rock.

entered the dry gas generation stage relatively quickly; the Weiyuan tectonic belt of the central Paleo-uplift entered the threshold of hydrocarbon generation earlier than the northeast part of the central Paleo-uplift, but entered the peak oil generation earlier in the Early-Middle Permian. Therefore, tectonic and sedimentary burial together with high heat flow values caused by the eruption of the Emeishan basalt in the Late Permian were main factors controlling levels of thermal maturity of the Qiongzhusi Formation. The present-day over-mature of the Qiongzhusi Formation is controlled by continuous subsidence since the Triassic, which means that the residual thickness of the Mesozoic strata combined with the last stage denudation directly affects the maturity of the Qiongzhusi Formation.

Credit author statement

Qiu Nansheng: Conceptualization, Methodology, Writing – original draft, Writing – review & editing, Supervision, Project administration and Funding acquisition. **Liu Wen**: Software, Formal analysis, Writing – original draft. **Fu Xiaodong**: Investigation, Resources. **Li Wenzheng:** Resources. **Xu Qiuchen**: Data curation, Writing – original draft. **Zhu Chuanqing**: Data curation

Declaration of competing interest

The authors declare that they have no known competing financial interests or personal relationships that could have appeared to influence the work reported in this paper.

Acknowledgments

The National Natural Science Foundation of China (Grant nos. 41830424, 41690133) and National key R & D projects (Grant no. 2017YFC0603102) provided financial support. Southwest Oil and Gas Field Branch, CNPC and SINOPEC provided geological data. The Platte River Assoc. provided BasinMod software for our maturation modeling.

References

Aldega, L., Bigi, S., Carminati, E., Trippetta, F., Corrado, S., Kavoosi, M.A., 2018. The Zagros fold-and-thrust belt in the Fars province (Iran): II. Thermal evolution. Mar. Petrol. Geol. 93, 376–390.

Balestra, M., Corrado, S., Aldega, L., Morticelli, M.G., Sulli, A., Rudkiewicz, J.C., Sassi, W., 2019a. Thermal and structural modeling of the Scillato wedge-top basin source-to-sink system: insights into the Sicilian fold-and-thrust belt evolution (Italy). Geol. Soc. Am. Bull. 131 (11/12), 1763–1782.

Balestra, M., Corrado, S., Aldega, L., Rudkiewicz, J.C., Morticelli, M.G., Sulli, A., Sassi, W., 2019b. 3D structural modeling and restoration of the Apennine-Maghrebian chain in Sicily: application for non-cylindrical fold-and-thrust belts. Tectonophysics 761, 86–107.

Bethke, C.M., 1985. A numerical model of compaction-driven groundwater flow and heat transfer and its application to the paleohydrology of intracratonic sedimentary basins. J. Geophys. Res. 90 (B8), 6817–6828.

Cao, H., Zhu, C., Qiu, N., 2015. Thermal evolution of lower silurian longmaxi Formation in the eastern Sichuan Basin. J. Earth Sci. Environ. 37 (6), 22–32.

Cao, H., Zhu, C., Qiu, N., 2016. Maximum paleotemperature of main paleozoic argillutite in the eastern Sichuan Basin. Chin. J. Geophys. 59 (3), 1017–1029 (in Chinese with English abstract).

Deng, B., Liu, S.G., Li, Z.W., Jansa, L.F., Liu, S., Wang, G.Z., Sun, W., 2013. Differential exhumation at eastern margin of the Tibetan Plateau, from apatite fission-track thermochronology. Tectonophysics 591, 98–115.

Du, J., Wang, Z., Zou, C., Xu, C., Shen, P., Zhang, B., Jiang, H., Huang, S., 2016. Discovery of intra-cratonic rift in the Upper Yangtze and its control effect on the formation of Anyue giant gas field. Acta Pet. Sin. 37 (1), 1–16 (in Chinese with English abstract).

He, B., X, Y., Chung, S., et al., 2003. Sedimentary evidence for a rapid, kilometer-scale crustal doming prior to the eruption of the Emeishan flood basalts. Earth Planet Sci. Lett. 213, 391–405.

He, D., Li, D., Zhang, G., Zhao, L., Fan, C., Lu, R., Wen, Z., 2011a. Formation and evolution of multi-cycle superposed Sichuan Basin, China. Chin. J. Geol. 46 (3), 589–606.

He, L., Xu, H., Wang, J., 2011b. Thermal evolution and dynamic mechanism of the Sichuan Basin during the early permian-middle triassic. Sci. China Earth Sci. 41 (12), 1884–1891 (in Chinese with English abstract).

He, L., Huang, F., Liu, Q., Li, C., Wang, J., 2014. Tectono-thermal evolution of Sichuan Basin in early paleozoic. J. Earth Sci. Environ. 36 (2), 10–17 (in Chinese with English abstract).

Huang, F., Liu, Q., He, L., 2012. Tectono-thermal modeling of the Sichuan Basin since the late Himalayan period. Chin. J. Geophys. 55 (11), 3742–3753 (in Chinese with English abstract).

Jiang, Q., Qiu, N., Zhu, C., 2018. Heat flow study of the Emeishan large igneous province region: implications for the geodynamics of the Emeishan mantle plume. Tectonophysics 724–725, 11–27.

Jiang, Q., Zhu, C., Qiu, N., 2015. Paleo-heat flow and thermal evolution of the lower cambrian Qiongzhusi shale in the southern Sichuan Basin, SW China. Natl. Gas Geosci. 26 (8), 1563–1570.

Li, D., Guo, T., Jiang, X., Zhao, H., Wang, H., 2015. Erosion thickness recovery and tectonic evolution characterization of southern East China Sea Shelf Basin. Oil Gas Geol. 36 (6), 913–923 (in Chinese).

Li, X., Li, Z., Sinclair, J.A., Li, W., Carter, G., 2006. Revisiting the "yanbian terrane": implications for neoproterozoic tectonic evolution of the western Yangtze block, south China. Precambrian Res. 151 (1–2), 14–30.

Li, M.J., Wang, T.G., Chen, J.F., He, F.Q., Yun, L., Akbar, S., Zhang, W.B., 2010. Paleo-heat flow evolution of the Tabei uplift in Tarim Basin, northwest China. J. Asian Earth Sci. 37, 52–66.

Li, X., Zhang, J., Wang, Y., Zhao, P., Wang, Z., Xu, H., Wang, G., Wang, F., 2016. Accumulation conditions of lower paleozoic shale gas from the southern Sichuan Basin, China. J. Natl. Gas Geosci. 1, 101–108.

Liang, D., Guo, T., Chen, J., Bian, L., Zhao, Z., 2008. Distribution of four suits of reginal marine source rocks. Mar. Origin Petrol. Geol. 13 (2), 1–16.

Liu, S., Deng, B., Li, Z., Sun, W., 2012. Architecture of basin-mountain systems and their influences on gas distribution: a case study from the Sichuan basin, South China. J. Asian Earth Sci. 47, 204–215.

Liu, S., Sun, W., Zhong, Y., Deng, B., Song, J., Ran, B., Luo, Z., Han, K., 2017. Evolutionary episodes and their characteristics within the Sichuan marine craton basin during Phanerozoic Eon, China. Acta Petrol. Sin. 33 (4), 1058–1072.

Liu, W., Qiu, N., Xu, Q., Liu, Y., 2018. Precambrian temperature and pressure system of Gaoshiti-Moxi block in the central paleo-uplift of Sichuan Basin, southwest China. Precambrian Res. 313, 91–108.

Liu, Y., Qiu, N., Xie, Z., Yao, Q., Zhu, C., 2016. Overpressure compartments in the central paleo-uplift, Sichuan Basin, southwest China. AAPG (Am. Assoc. Pet. Geol.) Bull. 100 (5), 867–888.

Lu, Q., Gu, T., Hu, S., 2006. Hydrothermal history and hydrocarbon generation history in northeastern Sichuan Basin. Xinjiang Petroleum Geology 27 (5), 49–551.

Luo, B., Yang, Y., Luo, W., Wen, L., Wang, W., Chen, K., 2017. Controlling factors of Dengying Formation reservoirs in the central Sichuan paleo-uplift. Petrol. Res. 2, 54–63.

Ma, D., Qiu, N., Xu, W., Xie, Z., 2012. Distribution and evolution characteristic of favorable geothermal field for oil cracking gas in Sichuan Basin. J. Earth Sci. Environ. 34 (2), 49, 46.

Ma, Y., Guo, X., Guo, T., Huang, R., Cai, X., Li, G., 2007. The Puguang gas field: new giant discovery in the mature Sichuan Basin, southwest Chia. AAPG Bull. 91, 627–643.

Mei, Q.H., He, D.F., Wen, Z., Li, Y.Q., Li, J., 2014. Geologic structure and tectonic evolution of Leshan-Longnvsi paleo-uplift in Sichuan Basin, China. Acta Petrol. Sin. 35 (1), 11–25 (in Chinese).

Nielsen, S., Clausen, O., McGregor, E., 2017. Basin%Ro: a vitrinite reflectance model derived from basin and laboratory data. Basin Res. 29 (S1), 515–536.

Omodeo, S., Ondrak, S., Arribas, J., Mas, R., Guimerà, J., Martinez, L., 2019. Petroleum systems modeling in a fold-and-thrust belt setting: the inverted Cameros Basin, North-Central Spain. J. Petrol. Geol. 42 (2), 145–171.

Peters, K., Burnham, A., Walters, C., Schenk, O., 2018. Guidelines for kinetic input to petroleum system models from open-system pyrolysis. Mar. Petrol. Geol. 92, 979–986.

Qin, J., Wang, J., Qiu, N., 2008. Evidence of thermal evolution history of Northeast Sichuan Basin-(U-Th)/He low temperature thermochronometry of apatite and zircon. J. China Univ. Geosci. 19 (6), 591–601.

Qiu, N., Qin, J., McInnes, B., Wang, J., Tenger Zhen, L., 2008. Tectonothermal evolution of the northeastern Sichuan Basin: constraints from apatite and zircon (U-Th)/He ages and vitrinite reflectance data. Geol. J. China Univ. 14 (2), 223–230 (in Chinese with English abstract).

Qiu, N., Chang, J., Zuo, Y., Wang, J., Li, H., 2012. Thermal evolution and lower paleozoic source rocks maturation in the tarim basin, northwest China. AAPG (Am. Assoc. Pet. Geol.) Bull. 96 (5), 789–821.

Rao, S., Zhu, C., Wang, Q., Tang, X., Li, W., Jiang, G., Hu, S., Wang, J., 2013. Thermal evolution patterns of the Sinian-Lower Paleozoic source rocks in the Sichuan basin, southwest China. Chin. J. Geophys. 56 (5), 1549–1559 (in Chinese with English abstract).

Ren, J., Zhao, L., Xu, Q., Zhu, J., 2016. Global tectonic position and geodynamic system of China. Acta Geol. Sin. 90 (9), 2100–2108 (in Chinese with English abstract).

Robert, A., Pubellier, M., Sigoyer, J.D.E., Vergne, J., Lahfid, A., Cattin, R., Findling, N., Zhu, J., 2010. Structural and thermal characters of the LongmenShan (sichuan, China). Tectonophysics 491, 165–173.

Rojas, V., Mescua, J., Folguera, A., Becker, T., Sagripanti, L., Fennell, L., Orts, D., Ramos, V., 2015. Evolution of the Chos Malal and Agrio fold and thrust belts, Andes of Neuquen: insights from structural analysis and apatite fission track dating. J. S. Am. Earth Sci. 64 (SI), 418–433.

Schito, A., Andreucci, B., Aldega, L., Corrado, S., Paolo, L.D., Szaniawski, M.Z.R., Jankowski, L., Mazzoli, S., 2018. Burial and exhumation of the western border of the Ukrainian Shield (Podolia): a multi-disciplinary approach. Basin Res. 30, 532–549.

Sclater, J.G., Christie, P.A.F., 1980. Continental stretching: an explanation of the post-mid-cretaceous subsidence of the central north sea basin. J. Geophys. Res. 85, 3711–3739.
Suggate, R.P., 1998. Relations between depth of burial, vitrinite reflectance and geothermal gradient. J. Petrol. Geol. 21, 5–32.
Sweeney, J., Burnham, A., 1990. Evaluation of a simple model of vitrinite reflectance based on chemical kinetics. AAPG (Am. Assoc. Pet. Geol.) Bull. 74 (10), 1559–1570.
Tian, Y., Kohn, B., Qiu, N., Yuan, Y., Hu, S., Gleadow, A., Zhang, P., 2018. Eocene to miocene out-of-sequence deformation in the eastern Tibetan plateau: insights from shortening structures in the Sichuan Basin. J. Geophys. Res. Solid Earth 123 (2), 1840–1855.
Tian, Y., Qiu, N., Kohn, B., Zhu, C., Hu, S., Gleadow, A., McInnes, B., 2012. Detrital zircon (U-Th)/He thermochronometry of the Mesozoic Daba Shan foreland basin, central China: evidence from timing of post-orogenic denudation. Tectonophysics 570–571, 65–77.
Wang, X., Yang, Z., Han, B., 2015. Superposed evolution of Sichuan Basin and its petroleum accumulation. Earth Sci. Front. 22 (3), 161–173.
Wang, Z., Wang, Y., Wu, B., Wang, G., Sun, Z., Xu, L., Zhu, S., Sun, L., Wei, Z., 2017. Hydrocarbon gas generation from pyrolysis of extracts and residues of low maturity solid bitumens from the Sichuan Basin, China. Org. Geochem. 103, 51–62.
Wei, G., Shen, P., Yang, W., Zhang, J., Jiao, G., Xie, W., Xie, Z., 2013. Formation conditions and exploration prospects of Sinian large gas fields, Sichuan Basin. Petrol. Explor. Dev. 40 (2), 129–138.
Wei, G., Yang, W., Du, J., Xu, C., Zou, C., Xie, W., Wu, S., Zeng, F., 2015. Tectonic features of Gaoshiti-Moxi paleo-uplift and its controls on the formation of a giant gas field, Sichuan Basin, SW China. Petrol. Explor. Dev. 42 (3), 257–265.
Xu, G., Yuan, H., Ma, Y., Liu, S., Cai, X., Wang, G., Pan, C., 2007. The source of Sinian and Lower-Paleozoic bitumen and hydrocarbon evolution in the middle and southeast of the Sichuan Basin. Acta Geol. Sin. 81 (8), 1143–1152 (in Chinese with English abstract).
Xu, H., Wei, G., Jia, C., Yang, W., Zhou, T., Xie, W., Li, C., Luo, B., 2012. Tectonic evolution of the Leshan-Longnüsi paleo-uplift and its control on gas accumulation in the Sinian strata. Petrol. Explor. Dev. 39 (4), 436–446.
Xu, Q., Qiu, N., Liu, W., Shen, A., Wang, X., 2018. Thermal evolution and maturation of sinian and cambrian source rocks in the central Sichuan Basin, southwest China. J. Asian Earth Sci. 164, 143–158.
Zhang, B., Zhao, Z., Zhang, S., Chen, J., 2007a. Discussion on marine source rocks thermal evolvement patterns in the Tarim basin and Sichuan basin, west China. Chin. Sci. Bull. 52 (S1), 141–149.
Zhang, L., Wei, G., Li, X., Wang, Z., Xiao, X., 2007b. The thermal history of Sinian-Lower Palaeozic high/over mature source rock in Sichuan Basin. Natl. Gas Geosci. 18 (5), 726–731 (in Chinese with English abstract).
Zhao, W., Wang, Z., Jiang, H., Fu, X., Xie, W., Xu, A., Shen, A., Shi, S., Huang, S., Jiang, Q., 2020. Exploration status of the deep Sinian strata in the Sichuan Basin: formation conditions of old giant carbonate oil/gas fields. Nat. Gas. Ind. 40 (2), 1–10 (in Chinese with English abstract).
Zhu, C., Xu, M., Shan, J., Yuan, Y., Zhao, Y., Hu, S., 2009. Quantifying the denudations of major tectonic events in Sichuan basin: constrained by the paleothermal records. Chin. Geol. 36 (6), 1268–1367 (in Chinese with English abstract).
Zhu, C., Tian, Y., Xu, M., Rao, S., Yuan, Y., Zhao, Y., Hu, S., 2010. The effect of Emeishan supper mantle plume to the thermal evolution of source rocks in the Sichuan Basin. Chin. J. Geophys. 53 (1), 119–127.
Zhu, C., Rao, S., Yuan, Y., Wang, Q., Qiu, N., Hu, S., 2013. Thermal evolution of the main paleozoic shale rocks in the southeastern Sichuan Basin. J. China Coal Soc. 38 (5), 834–839.
Zhu, C., Qiu, N., Jiang, Q., Hu, S., Zhang, S., 2015. Thermal history reconstruction based on multiple paleo-thermal records of the Yazihe area, western Sichuan depression. Chin. J. Geophys. 58 (10), 3660–3670 (in Chinese with English abstract).
Zhu, C., Hu, S., Qiu, N., Rao, S., Yuan, Y., 2016. Thermal history of the Sichuan Basin, SW China: evidence from deep boreholes. Sci. China (Earth Sci.) 56 (1), 70–80.
Zhu, C., Qiu, N., Cao, H., Liu, Y., Jiang, Q., 2017. Tectono-thermal evolution of the eastern Sichuan Basin: constraints from the vitrinite reflectance and apatite fission track data. Earth Sci. Front. 24 (3), 94–104.
Zhu, C., Hu, S., Qiu, N., Jiang, Q., Rao, S., Liu, S., 2018. Geothermal constraints on Emeishan mantle plume magmatism: paleotemperature reconstruction of the Sichuan Basin, SW China. Int. J. Earth Sci. 107, 71–88.
Zhu, C., Qiu, N., Liu, Y., Hu, S., 2019. Constraining the denudation process in the Eastern Sichuan Basin using low-temperature thermochronology and vitrinite reflectance data from boreholes. Geol. J. 54, 426–437.
Zou, C., Du, J., Xu, C., Wang, Z., Zhang, B., Wei, G., Wang, T., Yao, G., Deng, S., Liu, J., Zhou, H., Xu, A., Yang, Z., Jiang, H., Gu, Z., 2014a. Formation, distribution, resource potential, and discovery of Sinian-Cambrian giant gas field, Sichuan Basin, SW China. Petrol. Explor. Dev. 41 (3), 306–325.
Zou, C., Wei, G., Xu, C., Du, J., Xie, Z., Wang, Z., Hou, L., Yang, C., Li, J., Yang, W., 2014b. Geochemistry of the sinian-cambrian gas system in the Sichuan Basin, China. Org. Geochem. 74, 13–21.